



Review

Electrochemical (Bio)Sensors for Pesticides Detection Using Screen-Printed Electrodes

Beatriz Pérez-Fernández , Agustín Costa-García [†] and Alfredo de la Escosura- Muñiz ^{*}

NanoBioAnalysis Group-Department of Physical and Analytical Chemistry, University of Oviedo, Julián Clavería 8, 33006 Oviedo, Spain

^{*} Correspondence: alfredo.escosura@uniovi.es; Tel.: +34-985-103-521[†] In Memoriam to Prof. Agustín Costa-García.

Received: 12 March 2020; Accepted: 30 March 2020; Published: 2 April 2020



Abstract: Pesticides are among the most important contaminants in food, leading to important global health problems. While conventional techniques such as high-performance liquid chromatography (HPLC) and mass spectrometry (MS) have traditionally been utilized for the detection of such food contaminants, they are relatively expensive, time-consuming and labor intensive, limiting their use for point-of-care (POC) applications. Electrochemical (bio)sensors are emerging devices meeting such expectations, since they represent reliable, simple, cheap, portable, selective and easy to use analytical tools that can be used outside the laboratories by non-specialized personnel. Screen-printed electrodes (SPEs) stand out from the variety of transducers used in electrochemical (bio)sensing because of their small size, high integration, low cost and ability to measure in few microliters of sample. In this context, in this review article, we summarize and discuss about the use of SPEs as analytical tools in the development of (bio)sensors for pesticides of interest for food control. Finally, aspects related to the analytical performance of the developed (bio)sensors together with prospects for future improvements are discussed.

Keywords: screen-printed electrodes; electrochemical (bio)sensors; pesticides; point-of-care; food control

1. Introduction

Pesticides are among the most used products in the agri-food industry for the control, prevention and elimination of pests. According to the target pest, they can be classified in insecticides, acaricides, fungicides, bactericides, herbicides, etc. The main pesticides are made of carbamates, dinitrocompounds, organochlorines, organophosphates, pyrethroids, neonicotinoids or triazines, among others [1]. However, such compounds have a high toxicity. In this line, according to the World Health Organization (WHO), they can be classified as carcinogenic, neurotoxic or teratogenic [2,3]. This makes necessary their strict control in wastewater, soil, food, animals and human beings. In the European Union, the Residual Maximum Limits (MRLs) allowed by the legislation are 0.1 µg/L for individual pesticides and 0.5 µg/L for total pesticides [4–6].

The United Nations (UN) estimates that 200,000 deaths from acute poisoning occur each year due to pesticides, 99% belonging to developing countries [7]. Continuous exposure to these compounds may cause cancer, Alzheimer's disease and Parkinson's disease, as well as neurological disorders, fertility issues, allergies and hypersensitivity.

The official methods for the determination of pesticides are based on chromatography, such as High Performance Liquid Chromatography (HPLC), HPLC-MS/MS and Gas Chromatography coupled to Mass Spectrometry (GC-MS/MS) [8–13]. Despite their high sensitivity, these techniques require very expensive equipment, long analysis times, high reagent sample volumes and qualified

personnel. Due to these limitations, alternative methodologies for pesticides detection have been proposed in the last years, being probably the most relevant ones those based on electrochemical methods [14]. Electrochemical techniques have advantages over conventional ones related to their simplicity, the low sample volumes required (typically in the order of μL), the low cost of instruments and the short analysis time [15,16]. The main (bio)sensing routes for the electrochemical detection of pesticides are based on (Figure 1): (i) enzymatic sensors (inhibition and enzymatic catalysis); (ii) direct detection-based sensors (of electroactive pesticides); (iii) immunosensors (using specific antibodies as receptors); (iv) aptasensors (using specific aptamers as receptors) and (v) biological sensors (using microorganisms as receptors).

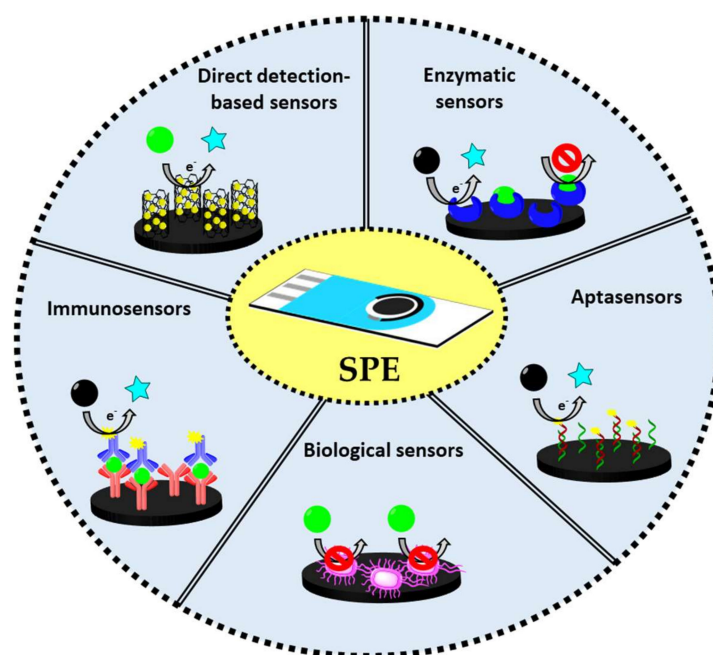


Figure 1. Main (bio)sensing routes followed for the electrochemical detection of pesticides.

However, the use of traditional electrodes requires relatively high sample volumes and quite complicated cell set-up, as they are not suitable for “in field” applications. In this sense, screen-printed electrodes (SPEs) have emerged as outstanding alternatives, overcoming the limitations of traditional electrodes. Screen printing is a well-developed technology widely used since the 1990s for the mass production of disposable and economical electrochemical sensors. This production process is carried out in several stages, as illustrated in Figure 2A [17].

Screen-printed electrodes (SPEs) are manufactured on ceramic or plastic substrates, in which different types of inks (typically carbon, graphite, silver and gold) are printed. In addition, these inks can be modified with nanomaterials or enzymes among other compounds, improving the analytical characteristics of the (bio)sensors developed from such electrodes.

SPEs satisfy the need for highly reproducible, sensitive and cost-effective detection methods, with additional advantages related to the low cost of production, flexibility in design, small size and ease of electrode surface modification [18–23]. The main methods used for the immobilization of (bio)receptors on the working electrode of SPEs for further pesticides detection are summarized in Figure 2B. The portability of the electrochemical instruments typically used also makes these systems ideal for point of care (POC) analysis [24–27]. The working electrode can be modified with various materials and recognition elements such as noble metal nanoparticles (i.e., Cu, Ni, Au, Pt, Ag) [28–37], nanotubes (CNT) [38–44], nanofibers (CNF) [43,45–49], graphene [50], graphene oxide (GO) [51–54], reduced graphene oxide (rGO) [55–58], quantum dots (QDs) [59–64], magnetic beads (MB) [65–68], enzymes

(AChE, ALP, GOD, HRP, FDH, OPH, Tyr) [69–80], antibodies [81–87], aptamers [88–93], DNA [94–98] and biological agents [99–101].

In this review, recent applications of SPEs for the electrochemical detection of pesticides are summarized, giving a critical vision on the advantages, drawbacks and perspectives.

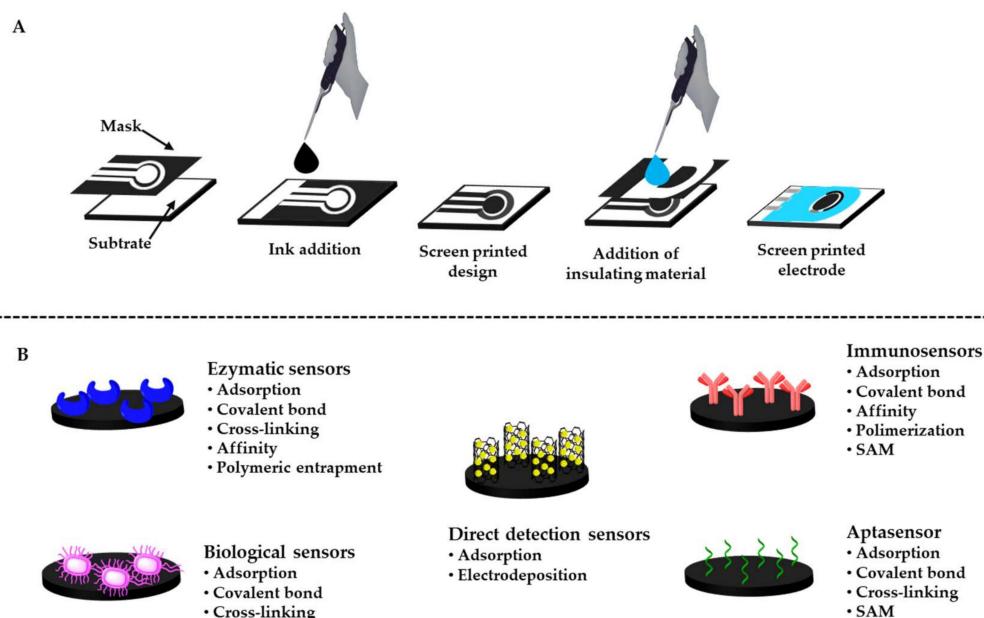


Figure 2. (A) Stages of the manufacturing process of screen-printed electrodes (SPEs). (B) Main methods used for the immobilization of (bio)receptors on the working electrode of SPEs for pesticides detection (SAM: Self Assembled Monolayers).

2. Electrochemical Techniques Used for Pesticides Detection

The typical electrochemical techniques used for pesticides detection, after following one of the (bio)sensing routes schematized in Figure 1, are: voltammetry (cyclic voltammetry, differential pulse voltammetry, square wave voltammetry), chronoamperometry and electrochemical impedance spectroscopy. The main characteristics of each technique are briefly described in this section.

2.1. Cyclic Voltammetry

Cyclic voltammetry (CV) is used to study the different electrochemical processes that take place when applying a potential scan. The measured peaks of current provide information on the oxidation and reduction processes of an electroactive specie. In addition, it provides information on the type of process object of study: (i) reversible; (ii) irreversible or (iii) quasi-reversible, depending on the separation between the anodic and cathodic peaks. Another characteristic that popularizes the CV is its ability to give information about the nature of a process in terms of adsorption and diffusion characteristics.

2.2. Differential Pulse Voltammetry

Differential pulse voltammetry (DPV) technique consists in applying a sequence of pulses of constant amplitude superimposed on a stepped potential increase. The current intensity is measured just before applying the pulse and at the end of it. The response obtained is the difference between the two current intensities, in relation to the potential at the start of the pulse, giving rise to a peak-like response.

This technique is used to determine oxidation or reduction processes depending on the analyte concentration. In general terms, DPV has better sensitivity than cyclic voltammetry.

2.3. Square Wave Voltammetry

In square wave voltammetry (SWV) technique, a large amplitude square wave potential sweep is applied with a stepped potential ramp. Current intensity is measured at the end of each applied pulse in the potential sweep cycle.

Generally, SWV is more sensitive, faster and more selective than DPV, since the background current is minimized.

2.4. Chronoamperometry

Chronoamperometry (AC) is a determination technique where a constant current intensity is applied for a certain time. During to the application of such potential, the electroactive analytes present in the solution are oxidized or reduced, generating and associated current, proportional to the amount of analyte. The main advantage of this technique compared with voltammetries is related to its simplicity.

2.5. Electrochemical Impedance Spectroscopy

Electrochemical impedance spectroscopy (EIS) is a technique commonly used to evaluate parameters of charge transfer, corrosion processes, double-layer formation, or modification processes of the electrode surface.

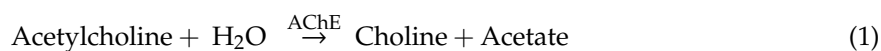
The EIS is given by the Nyquist diagram where values of the load transfer resistance and the resistance of the solution are obtained. Depending on the semicircle obtained in the Nyquist diagram, it can be determined if there is an impediment to the charge transfer or if it is favored by the modification of the working electrode. This technique is widely used in label-free biosensing formats, where the change in the impedance upon the analyte biorecognition allows its determination.

3. Enzymatic Sensors

Enzymatic sensors are the most widely used for the determination of pesticides on SPEs. Two are the main detection routes based on enzymes: (i) enzymatic inhibition route, where the pesticide inactivates the enzyme and (ii) catalytic route, where the pesticide is hydrolyzed by the enzyme generating an electroactive compound [102,103].

3.1. Enzymatic Inhibition

As stated above, inhibition reactions make enzymes inactive in the presence of pesticides. This is the case of acetylcholinesterase (AChE), butyrylcholinesterase (BChE), tyrosinase (Tyr) and alkaline phosphatase (ALP).



AChE is one of the most commonly used enzymes for the determination of organophosphorus pesticides (OP). The reaction catalyzed by AChE is the following:

The presence of OP results in the inhibition of the enzymatic activity due to phosphorylation of the serine residue of the active center of the enzyme, which blocks the hydrolysis of acetylcholine (ACh). Therefore, the higher the concentration of OP, the more blocked the active center will be and the lower the signal of oxidation or reduction of the enzymatic products. Detection based on other enzymes relies in the same principles.

As shown in Table 1, many publications on enzymatic inhibition-based detection of pesticides on SPEs have been reported in the last years. For example, Solna et al. [74] developed a multi-analyte device for pesticides and phenols based on the immobilization of enzymes (AChE, BChE, Tyr, HRP) on different graphite and platinum working electrodes. AChE and BChE were immobilized on platinum working electrodes while Tyr and HRP did on graphite working electrodes. The limits of detection (LoDs) for the different pesticides studied depended on whether AChE or BChE were

used, ranging from 0.8 to 130 nM for AChE and 2.8 to 2390 nM for BChE. Such difference in LoDs is related to the different affinity of each enzyme for the corresponding pesticide. Industrial wastewater was successfully analyzed with such system. Another biosensor based on the inhibition of AChE on screen-printed carbon electrodes (SPCEs) was the developed by Dou et al. [104], where after the manufacturing of the SPCEs, the enzyme was immobilized by polyacrylamide polymerization. Dichlorvos, Monocrotophs and Parathion pesticides were determined with LoD of 18.1, 26.4 and 14.4 nM respectively. In both works the enzymes were immobilized on unmodified working electrodes, giving rise to simple and fast sensors.

Table 1. Enzyme inhibition biosensors reported for pesticides detection on screen-printed electrodes.

Electrode	Enzyme	Analyte	Lineal Range	LoD	Ref
SPGE (array)	AChE	Carbaryl Heptenophos Fenitrothion Dichlorvos Phosphamide	0.8 nM–2.4 µM	0.80 nM 9.2 nM 85 nM 77 nM 130 nM	[74]
	BChE	Carbaryl Heptenophos Fenitrothion Dichlorvos Phosphamide		93 nM 2.8 nM 6.9 nM 14 nM 2390 nM	
Thick-film SPCE	Tyr	Diethylidithio carbamate	–	2 µM	[79]
SPCE	AChE	Dichlorvos Monocrotophs Parathion	16–28 nM	18.1 nM 26.4 nM 14.4 nM	[104]
PB/SPCE	AChE	Aldicarb Carbaryl	63–315 nM 124–497 nM	63 nM 124 nM	[105]
	BChE	Paraoxon Chlorpyrifos-methyl oxon	7–18 nM 1.6–6 nM	7 nM 1.6 nM	
PEDOT:PSS/SPGE	AChE	Chlorpyrifos-oxon	4–760 nM	4.4 nM	[106]
TCNQ/SPGE	AChE	Aldicarb	10–500 nM	8 nM	[107]
		Carbaryl	5–500 nM	4 nM	
		Carbofuran	1–750 nM	1 nM	
		Methomyl	2.5–700 nM	2 nM	
CoPc/SWCNTs/ SPCE	AChE	Paraoxon Malaoxon	18–181 nM 6–159 nM	11 nM 6 nM	[108]
GA/ZnONPs/ SPCE	Tyr	Chlortoluron	1–100 nM	0.47 nM	[109]
Fe ₃ O ₄ /GR/SPCE	AChE	Chlorpyrifos	0.14–285 nM	0.06 nM	[110]
Al ₂ O ₃ /SPCE	AChE	Dichlorvos	1–60 µM	0.8 µM	[111]
CB/CoPc/SPCE	BChE	Paraoxon	Up to 100 nM	18 nM	[112]
CoPc/SPCE	AChE	Organophosphates	10 ^{−5} –10 ^{−9} M	–	[113]
Cyst/GA/AuSPE	AChE	Paraoxon	Up to 145 nM	7.3 nM	[114]
CoPc/CGCE	Tyr	Methyl parathion	22.8–379.9 nM	–	[115]
		Diazinon	62.4–164.3 nM		
		Carbofuran	22.6–406.8 nM		
		Carbaryl	49.7–248.5 nM		
Nf/SPGE	BChE	Trichlorfon Coumaphos	4 × 10 ^{−7} –8 × 10 ^{−7} M 2 × 10 ^{−7} –5.5 × 10 ^{−6} M	3.5 × 10 ^{−7} M 1.5 × 10 ^{−7} M	[116]
PB/SPGE	ChO	Paraoxon	0.1–1 µM	0.1 µM	[117]
DEP-Au chips	AChE	Paraoxon Carbofuran	–	36.3 nM 36.1 nM	[118]
GA/IrOxNPs/ SPCE	Tyr	Chlorpyrifos	0.01–0.1 µM	3 nM	[119]
SPCE	AChE	Chlorpyrifos	1 × 10 ^{−6} –5 × 10 ^{−2} M	5 µM	[120]
DCHP/MWCNT/SPCE	AChE	Chlorpyrifos	0.14–2.85 nM	0.14 nM	[121]
Nf/PB/DSPCE	AChE	Isocarbophos Chlorpyrifos Trochlorfon	0.33–16.72 µM	0.33 µM	[122]

Table 1. Cont.

Electrode	Enzyme	Analyte	Lineal Range	LoD	Ref
SPCE	AChE	Permethrin	6.2–41 μ M	8.1 μ M	[123]
Cu ₃ (PO ₄) ₂ /HNFs/SPCE	AChE/ ChO	Paraoxon	2.18 $\times 10^{-5}$ –2.18 nM	21.8 fM	[124]
GA/Nf/BSA/CBNPs/SPCE	BChE	Paraoxon	18.2–109 nM	18.2 nM	[125]
Nf/PB/ZrO ₂ /CNT/SPCE	GMP-AChE	Dimethoate	0.004–43.6 nM	2 pM	[126]
TCNQ/SPCE	BChE	Chlorpyrifos-methyl Coumaphos Carbofuran	3 $\times 10^{-8}$ –3 $\times 10^{-7}$ M 1 $\times 10^{-7}$ –4 $\times 10^{-6}$ M 3 $\times 10^{-8}$ –1 $\times 10^{-7}$ M	20nM 50 nM 10 nM	[127]
PB/SPCE	AChE/ ChO	Chlorpyrifos-methyl Carbofuran	4 $\times 10^{-8}$ –5 $\times 10^{-7}$ M 1 $\times 10^{-8}$ –1 $\times 10^{-7}$ M	30 nM 8 nM	[127]
MWCNTs/SnO ₂ /CHIT/SPCE	AChE	Chlorpyrifos	0.14–2.85 $\times 10^3$ nM	< 0.14 nM	[128]
CS/PVA NFM/SPCE	AChE	Pirimiphos-methyl oxon	1 $\times 10^{-10}$ –8 $\times 10^{-9}$ M	0.2 nM	[129]
OMC-CHIT/Fe ₃ O ₄ -CS/SPCE	AChE	Methamidophos Chlorpyrifos	–	7.09 nM 0.14 nM	[130]
SPSE	AChE	Chlorpyrifos	0–71.3 nM	7.13 nM	[131]
CS/CB/SPCE	AChE	Paraoxon	0.36–1.82 nM	0.18 nM	[132]
MWCNT/SPCE	AChE	Paraoxon	Up to 6.9 nM	0.5 nM	[132]
ZnO/SPCE	AChE	Paraoxon	Up to 5 μ M	0.13 μ M	[133]
SPGE	AChE	Chlorpyrifos ethyl oxon	0–2 $\times 10^{-8}$ M 5 $\times 10^{-8}$ –2 $\times 10^{-7}$ M	3.6 pM	[134]
MWCNT/IL/ SPCE	AChE	Chlorpyrifos	0.14–2.85 $\times 10^5$ nM	0.14 nM	[135]
PBNCs/rGO/ SPCE	AChE	Monocrotophos	4.5–2688 nM	0.45 nM	[136]
TCNQ/SPGE	AChE	Carbaryl Carbofuran Pirimicard	Up to 5 $\times 10^{-7}$ M Up to 1 $\times 10^{-7}$ M Up to 5 $\times 10^{-7}$ M	10 nM 0.8 nM 0.2 nM	[137]
CoPc/SPCE	AChE	Carbofuran	10 ⁻¹⁰ –10 ⁻⁸ M	0.5 nM	[138]
TCNQ/Nf/SPGE	AChE	Chlorpyrifos methyl	3–930 nM	68 nM	[139]
TCNQ/BSA/GA/SPCE	AChE	Paraoxon	1.8 $\times 10^{-7}$ –5.4 $\times 10^{-5}$ M	0.18 μ M	[140]
TCNQ/Nf/SPCE	AChE	Carbaryl Parathion methyl	9.9–447.3 nM 3.8–379.9 nM	9.9 nM 3.8 nM	[141]
CoPc/SPCE	AChE	Dichlorvos Parathion Azinphos	1 $\times 10^{-17}$ –1 $\times 10^{-4}$ M 1 $\times 10^{-16}$ –1 $\times 10^{-4}$ M 1 $\times 10^{-16}$ –1 $\times 10^{-4}$ M	fM 0.1 fM 0.1 fM	[142]

SPGE: Screen-printed graphite electrode; PB: Prussian Blue; PEDOT: Poly (3,4-ethylenedioxythiophene); PSS: Poly(styrene sulfonate); TCNQ:7,7',8,8'-Tetracyanoquinodimethane; GR: Graphene; Cyst: Cysteamine; GA: Glutaraldehyde; AuSPE: Screen-printed gold electrode; CGCE: Acetylcellulose-graphite composite electrode; Nf: Nafion; ChO: Choline oxidase; DEP: Disposable electrochemical printed; DCHP: Dicyclohexyl phthalate; DSPCE: Dual-channel screen-printed carbon electrode; GMP-AChE: Gold magnetic particles-Acetylcholinesterase; HNF: Hybrid nanoflowers; CBNP: Carbon black nanoparticles; CNT: Carbon nanotube; CHIT: Chitosan; PVA: Poly (vinyl alcohol); NFM: nanofibrous membranes; OMC-CHIT: ordered mesoporous carbon–chitosan; SPSE: Screen-printed silver electrode; IL: Ionic liquid; PBNC: Prussian Blue Nanocubes; rGO: reduced Graphene Oxide; BSA: Bovine Serum Albumin.

However, in most cases working electrodes are modified with different materials so as to improve the efficiency of the enzyme immobilization and thus the pesticide analysis. An example of simple electrode modification is the reported by Arduini et al. [105] where Prussian Blue was immobilized before the enzyme (AChE and BChE) did. The concentration of several organophosphorus pesticides was determined, finding the highest sensitivity for Aldicarb and Carbaryl (LoDs 63 and 124 nM respectively) when AChE was used and for Paraoxon and Chlorpyrifos-methyl oxon (LoDs 7 and 1.6 nM, respectively) when using BChE. River water and wastewater samples were analyzed with such biosensor. Polymers like poly (3,4-ethylenedioxythiophene) polycation (PEDOT) and poly (styrenesulfonate) polyanion (PSS) were also used for the carbon electrode modification so as to increase its conductivity [106]. Organophosphorus pesticides such as Chlorpyrifos-oxon were determined (LoD of 4.4 nM) based on the thiocholine oxidation. In the case of the biosensor

developed by Silva Nunes et al. [107], a screen-printed graphite electrode (SPGE) was modified with 7,7,8,8-tetracyanoquinodimethane (TCNQ) and photopolymerized with poly (vinyl alcohol) bearing styrylpyridinium groups (PVA-SbQ) to covalently immobilize AChE. This biosensor was applied for the determination of different carbamates such as Aldicarb (LoD 8 nM), Carbaryl (LoD 4 nM), Carbofuran (LoD 1 nM) and Methomyl (LoD 2 nM).

Different nanomaterials have also been proposed for the electrode's modification. For example, multi-walled carbon nanotubes (MWCNTs) were immobilized together with AChE and Co-phthalocyanine (Co-Pc; used as mediator) on the working electrode of a SPCE [108]. Such modification produces a decrease in the working potential, minimizing interferences and thus improving the selectivity of the biosensor. This device was developed for the determination of Paraoxon (LoD 11 nM) and Malaoxon (LoD 6 nM), even in tap and sparkling water. Metallic nanoparticles (NPs) have also been used as modifiers of the working electrode. This is the case of the Clortoluron sensing device developed by Haddaoui and Raouafi [109] using ZnO nNPs-modified electrodes for the immobilization of tyrosinase (Tyr) enzyme (Figure 3). Clortoluron is detected here with a LoD of 0.47 nM, having also a good performance in tap water, well water and river water. The stability of immobilized AChE as well as the electronic transference were also improved using magnetic nanoparticles (Fe_3O_4) coupled to a graphene (GR) film on a SPCE [110]. This biosensor was applied for the determination of Chlorpyrifos at levels of 0.06 nM even in vegetable samples (spinach and cabbage).

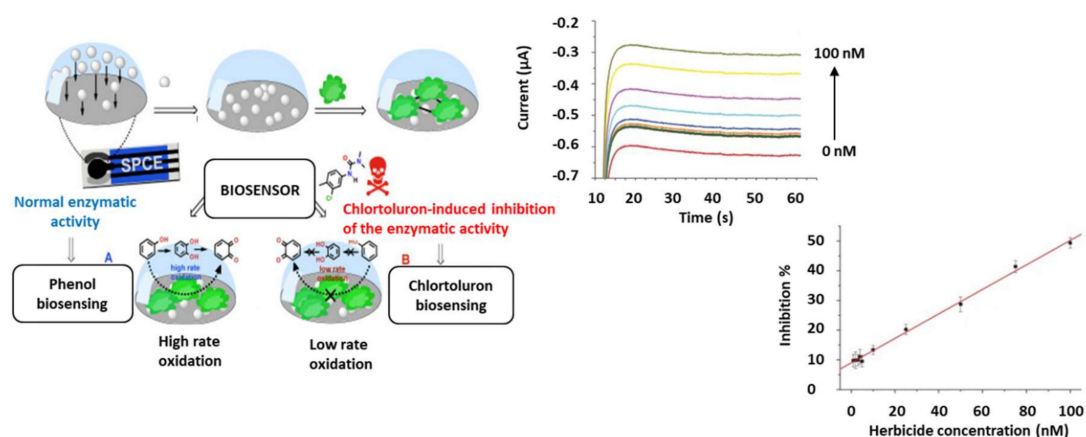


Figure 3. Enzyme inhibition biosensors for pesticides detection on screen-printed electrodes. (Left) scheme of a biosensor for Chlortoluron using a SPCE modified with ZnO NPs for Tyr enzyme immobilization; (Right) Chronoamperometric (CA) responses and calibration curve of inhibition % vs. concentration of herbicide. Reprinted from [109], Copyright 2015, with permission from Elsevier.

Alternatively, enzymes can also be trapped in gel matrices with which the electrode is subsequently modified. This is the case of the work developed by Shi et al. [111] where AChE is trapped in a sol-gel matrix of Al_2O_3 . Such matrix not only increases the stability of AChE but also catalyzes the oxidation of thiocholine, decreasing the working potential and minimizing interferences. Dichlorvos pesticide was determined at levels of 0.8 μM in river water samples.

As summarized in Table 1, the modification of SPEs with different materials highly improves the analytical characteristics of the biosensors, lowering at levels as low as the femtomolar scale.

3.2. Catalytic Detection

As stated above, an alternative route for pesticides detection using enzyme receptors is based on the pesticide hydrolysis by the enzyme generating an easily detected electroactive compound. Organophosphorus anhydrolase acid (OPAA) and organophosphorus hydrolase (OPH) are the main enzymes used for such purpose [143–147]. The OPAA is a more restrictive enzyme with respect to

organophosphorus compounds, being only able of catalyzing P-F bonds, while OPH also catalyzes organophosphorus containing P-O, P-S and P-CN bonds [148]. Therefore, OPH has a broader range of catalytic effect, being used to develop biosensors for total organophosphorus pesticides.

The catalytic reaction of OP through the use of OPH gives rise to the electroactive p-nitrophenol product. Consequently, the amount of OP is proportional to the production of p-nitrophenol. The generic reaction catalyzed by OPH is as follows:



Table 2 summarizes the different biosensors reported for organophosphates detection based on enzymatic hydrolysis. As in the case of the enzymatic inhibition, different materials have been evaluated for the electrode modification so as to improve the performance of the biosensor.

Table 2. Enzymatic hydrolysis-based biosensors reported for pesticides detection on screen-printed electrodes.

Electrode	Enzyme	Analyte	Lineal Range	LoD	Ref
Nf/SPCE	OPH	Paraoxon Methyl parathion	4.6–46 μM Up to 5 μM	0.9 μM 0.4 μM	[148,149]
MWCNT/SPCE	OPH	Demeton-S	Up to 85 μM	1 μM	[150]
Fe_3O_4 @Au-NC/ SPCE	MPH	Methyl parathion	1.9–3799 nM	0.38 nM	[151]
SPCE	PH	Parathion	34–343 nM	3.4 nM	[152]
BSA/GA/SPCE	OPH	Diazinon	–	0.59 μM	[153]

Nf: Nafion; OPH: Organophosphorus hydrolase; NC: Nanocomposite; MPH: Methyl parathion hydrolase; PH: Parathion hydrolase; GA: Glutaraldehyde.

As a representative example, Mulchandani et al. [149] modified the SPCE with Nafion (Nf) for the OPH immobilization and subsequent determination of Paraoxon and Methyl parathion in river water samples at 0.9 and 0.4 μM levels respectively. They and others [150], also evaluated the SPCE modification with MWCNT for the enzyme immobilization finding worse sensitivity than for the Nf-based modification.

Metallic NPs have also been proposed for the electrode modification. In particular, AuNPs surrounding the core of magnetic Fe_3O_4 NPs were used for the immobilization of methyl parathion hydrolase enzyme (MPH) which allowed the detection of Methyl parathion at levels as low as 0.38 nM (Figure 4) [151]. The use of the AuNP/ Fe_3O_4 NPs matrix also allowed to work at low potentials, minimizing interferences when analyzing river water samples.

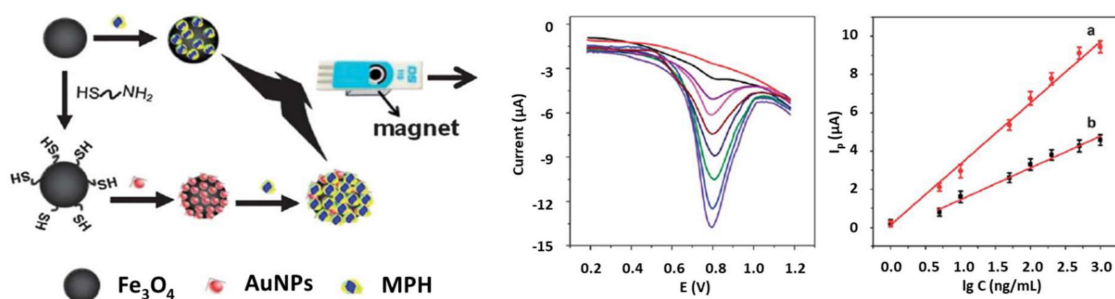


Figure 4. Enzymatic hydrolysis-based biosensors for pesticides detection on screen-printed electrodes. (Left) Scheme of an approach based on the SPCE modification with AuNPs/ Fe_3O_4 NPs for MPH immobilization and further determination of methyl parathion; (Right) SWV measurements of methyl parathion at different concentrations and calibration plots for the electrode with (a) and without (b) AuNPs. Reprinted from [151], Copyright 2013, with permission from Royal Society of Chemistry.

4. Direct Detection of Electroactive Pesticides

In spite of their advantages, the use of enzymes entails important limitations related to their low stability over time and their sensitivity to changes in temperature and pH [154]. Moreover, some pesticides are electroactive compounds able to be electrochemically detected without the need of enzymes [155,156]. For this reason, the growth of electrochemical sensors without enzymes is continuously increasing, benefiting of their lower cost, greater simplicity and faster analysis. However, in most cases the sensitivity of such direct detection on unmodified SPEs is not enough for detecting the pesticides at the maximum levels allowed by the legislation. Working electrode modification with different materials, mainly metallic nanoparticles (made of i.e., Ag, Zn, Cu, Ni) and carbon nanomaterials such as nanofibers (CNF), nanotubes (CNT) or graphene, etc. has been extensively studied so as to improve the electronic transference and thus the sensitivity of the pesticide detection.

Direct detection approaches for pesticides determination on SPEs are summarized in Table 3. As a representative example of direct detection without electrode modification, Geto et al. [157] self-prepared carbon made SPEs (SPCE) (Figure 5A) for the rapid determination of Bentazone (BTZN), an important herbicide used in agriculture. The voltammetric oxidation of the tertiary amine in the pesticide was selected as the analytical signal that allowed its quantification. A detection limit below the MRL (3.4 nM) was obtained, also demonstrating the good performance of the sensor in groundwater and lake water.

Table 3. Direct detection-based biosensors reported for pesticides determination on screen-printed electrodes.

Electrode	Analyte	Lineal range	LoD	Ref
SPCE	Bentazone	0.19–50 μ M	34 nM	[157]
CB/SPCE	Carbofuran	0.1–100 μ M	49 nM	[158]
	Isoproc carb	0.1–100 μ M	79 nM	
	Carbaryl	0.1–100 μ M	48 nM	
	Fenobucarb	0.1–100 μ M	80 nM	
Thick-film Bi/SPCE	Imidacloprid	0–110.26 μ M	2.97 μ M	[159]
	Thiamethoxam		2.68 μ M	
	Dinotefuran		7.67 μ M	
	Clothianidin		4.12 μ M	
	Nitenpyram		4.36 μ M	
NiO/SPCE	Parathion	0.1–5 μ M and 5–30 μ M	24 nM	[160]
AuNPs/SPCE	Thiram	0.29–62.39 μ M	90 nM	[161]
	DEDMTDS	0.15–26.62 μ M	50 nM	
	Disulfiram	1.69–50.58 μ M	550 nM	
MIP/AuNPs/ERGO/SPCE	Cyhexatin	2.60–1298.18 nM	0.52 nM	[162]
CoPc/SWCNT/SPGE	Thiocholine	0.07–0.45 mM	38 μ M	[163]
ZnONPs/MWCNTs/SPCE	Glyphosate	1–10 μ M	300 nM	[164]
		ZnONPs/Au-SPCE	10–100 μ M	
AG/AuNPs/SPCE	Hydrazine	0.002–936 μ M	0.57 nM	[165]
CHIT/ZnO/SPCE	4-nitrophenol	0.5–400.6 μ M	230 nM	[166]
Graphene/Nf/SPCE	4-nitrophenol	10–620 μ M	600 nM	[167]
		MWCNT/Nf/SPCE	25–620 μ M	
MWCNT-SPE	Sulfentrazone	1–30 μ M	150 nM	[168]
AuNP/CeO ₂ /SPGE	Hydrazine	0.01–10 mM	–	[169]
CuONPs/SPCE	DCMU	0.5–2.5 μ M	47 nM	[170]
NG-PVP/ AuNPs/SPCE	Hydrazine	2–300 μ M	70 nM	[171]
Nafion/CNT/SPCE	Paraquat	0.54–4.30 μ M	170 nM	[172]
AuNPs/GO/SPCE	Carbofuran	1–30 μ M	220 nM	[173]
		30–250 μ M		
Ag@GNRs/SPCE	Methyl parathion	0.005–2780 μ M	0.5 nM	[174]
CoHCF/SPGE	Thiocholine	5×10^{-7} – 1×10^{-5} M	500 nM	[175]
CB/CoPc/SPCE	Thiocholine	Up to 6 mM	4 μ M	[112]

CB: Carbon-black; NP: Nanoparticles; DEDMTDS: N,N-diethyl-N',N'-dimethylthiuram disulfide; CoPc: Cobalt phthalocyanine; SWCNT: Single-walled carbon nanotube; SPGE: Screen-printed graphite electrode; MWCNT: Multi-walled carbon nanotube; AMPA: Aminomethyl phosphoric acid; MIP: Molecularly imprinting polymer; ERGO: Electrochemical reduction graphene oxide; AG: Activ ated graphite; CHIT: Chitosan; Nf: Nafion; DCMU: 3-(3,4-dichlorophenyl)-1,1-dimethylurea; NG: Nitrogen-doped graphene; PVP: Polyvinylpyrrolidone; GNR: Graphene nanoribbons; CoHCF: Cobalt hexacyanoferrate.

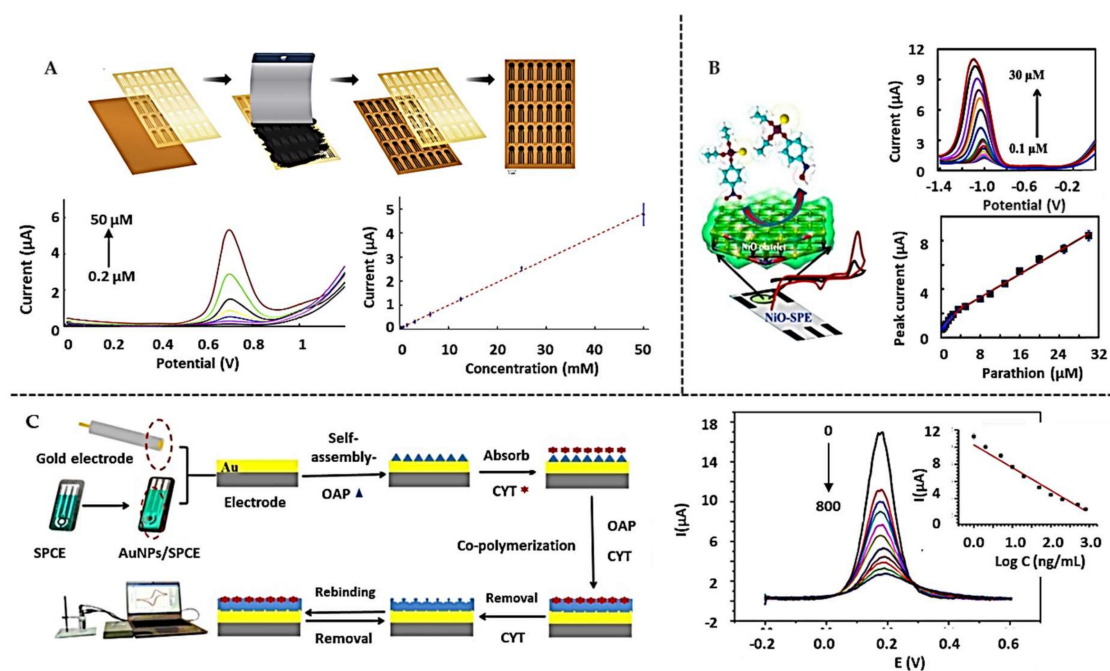


Figure 5. Direct detection-based biosensors for pesticides determination on screen-printed electrodes: (A) Scheme of the preparation of SPE for the determination of BTZN, SWV measurements and calibration curve. Reprinted from [157], Copyright 2019, with permission from Elsevier. (B) SPE modified with NiO NPs to determine Parathion, DPV signals and calibration curve. Reprinted from [160], Copyright 2018, with permission from Elsevier. (C) Use of MIP for the determination of CYT. Measurements by DPV and inset the calibration curve. Reprinted from [162], Copyright 2019, with permission from Elsevier.

However, as stated above, in most cases SPE modification is required for improving the sensor sensitivity. In this line, Della Pelle et al. [158] used black nanocarbon (CB) to develop a device for the determination of phenylcarbamates (i.e., Carbaryl, Carbofuran, Isoprocarb and Phenobcarb). In this case, the analytical signal corresponds to the voltammetric oxidation of the hydrolyzed forms of the pesticides, which allowed to reach LoD ranging from 48 to 80 nM. Wheat and corn samples were also analyzed after extraction and hydrolysis treatment.

Thick bismuth films have also been proposed as SPEs modifiers for the determination of neonicotinoid pesticides such as Clothianidin, Imidacloprid, Thiamethoxam and Nitenpyram [159]. The voltammetric reduction of the nitro group of the pesticides to hydroxylamine allowed the use of quantitative analysis, reaching LoDs at levels in the range 2.97–4.12 μM . Tap water, mineral water and samples from rivers and lakes were successfully analyzed.

NiO NPs have also been used to improve the sensitivity and stability for the determination of Parathion (Figure 5B) [160]. Such NPs catalyze the voltammetric reduction of the nitro group of the Parathion to hydroxylamine, allowing the detection of the pesticide at 24 nM levels. Tap water and human urine samples were analyzed without any pretreatment while a tomato juice sample only required a simple filtration.

AuNPs were also used to increase the electrode surface of the SPCE and catalyze the amperometric oxidation of Thiram, Disulfiram and N,N-diethyl-N',N'-dimethylthiuram disulfide (DEDMTS) pesticides [161]. Interestingly, in this case, this sensor was coupled to an Ultra High-Performance Liquid Chromatography (UHPLC) system to perform a previous separation and improve the selectivity. LoDs ranging from 0.05 to 0.55 μM were obtained with such system, also analyzing samples of apple, grape and lettuce after extraction, filtration and centrifugation.

The high selectivity given by the use of molecularly imprinted polymeric membranes (MIP) has also been approached for the specific pesticide detection. As an example, a MIP combined with AuNPs

and reduced graphene oxide (rGO), was used for the specific voltammetric determination of Cyhexatin (CYT) [162] (Figure 5C), reaching a LoD as low as 0.52 nM.

The SPEs electrodes used by Jubete et al. [163] were modified with single-wall carbon nanotubes (SWCNT) and cobalt phthalocyanine (CoPc) for the determination of Thiocholine (TCh), by monitoring its amperometric oxidation. This system gave a relatively low sensitivity with LoDs at 38 μ M levels. In contrast, when zinc oxide nanoparticles (ZnONP) were used in combination with multi-walled carbon nanotubes (MWCNTs) [164] for the determination of Glyphosate and its hydrolysis product (aminomethylphosphonic acid, AMPA) the LoDs were significantly better (300 nM and 3 μ M).

5. Immunosensors

Immunosensors for pesticides detection are based on the use of antibodies and antigens as recognition elements immobilized on the SPE. The main advantages of such biosensors over enzymatic ones rely on the higher stability of antibodies/antigens together with greater selectivity and specificity. However, the high cost and low availability of monoclonal antibodies is an important limitation that should be considered. The small size of the pesticides also usually avoids sandwich-based approaches, so competitive immunoassays are often required. Immunosensors for Imidacloprid, Parathion, Methyl Chlorpyrifos, Chlorsulfuron and Atrazine can be found in the literature, as shown in Table 4.

Table 4. Immunosensors reported for pesticides determination on screen-printed electrodes.

Electrode	Analyte	Lineal range	LoD	Ref
Ab/fG-SPCE	Parathion	0.3–3.43 $\times 10^3$ pM	0.18 pM	[176]
Ab/NH ₂ -GQD/SPCE	Parathion	0.03–3.43 $\times 10^6$ pM	0.16 pM	[177]
PO-SPCE	Chlorsulfuron	0.03–3.88 nM	30 pM	[178]
BSA-IMD/SPCE	Imidacloprid	50–10000 pM	24 pM	[179]
Ab/AuNP/SPCE	Imidacloprid	50–10000 pM	22 pM	[180]
BSA-Ag/Pt/SiO ₂ /SPCE	Chlorpyrifos methyl	1.24–62 nM	70 pM	[181]
Ab/PANI/PVS/SPCE	Atrazine	0.02–0.22 μ M	4.6 nM	[182]
Ab/ATPh/GA/AuSPE	2,4-D	45 nM–0.45 mM	–	[183]

Ab: Antibody; fG: functionalized graphene; PO: Peroxidase; BSA: Bovine serum albumin; IMD: Imidacloprid; GQD: Graphene Quantum Dots; Ag: Antigen; ATPh: 4-aminothiophenol; GA: Glutaraldehyde; AuSPE: Screen-printed gold electrode; 2,4-D: 2,4-dichlorophenoxyacetic acid.

In most cases, SPEs are modified with different (nano)materials so as to improve the efficiency of the receptor immobilization. As example, graphene sheets [176] and graphene quantum dots (GQDs) [177] modified with amino groups have been proposed for the oriented immobilization of antibodies on SPCE. In both cases, anti-parathion antibodies were immobilized for the further Parathion recognition and final detection by means of electrochemical impedance spectroscopy (EIS), reaching LoDs as low as 0.16 pM, with high selectivity even in tomato and carrot samples after extraction (Figure 6A).

Representative examples of competitive immunosensors are those based on the use of enzymatic tags proposed for the determination of Chlorsulfuron [178] and Imidacloprid [179] at levels as low as 22 pM, also taking advantage of the use of AuNPs [180] for the immobilization of the antibody. Tap water, watermelon and tomato samples were analyzed here without the need of pretreatment (Figure 6B).

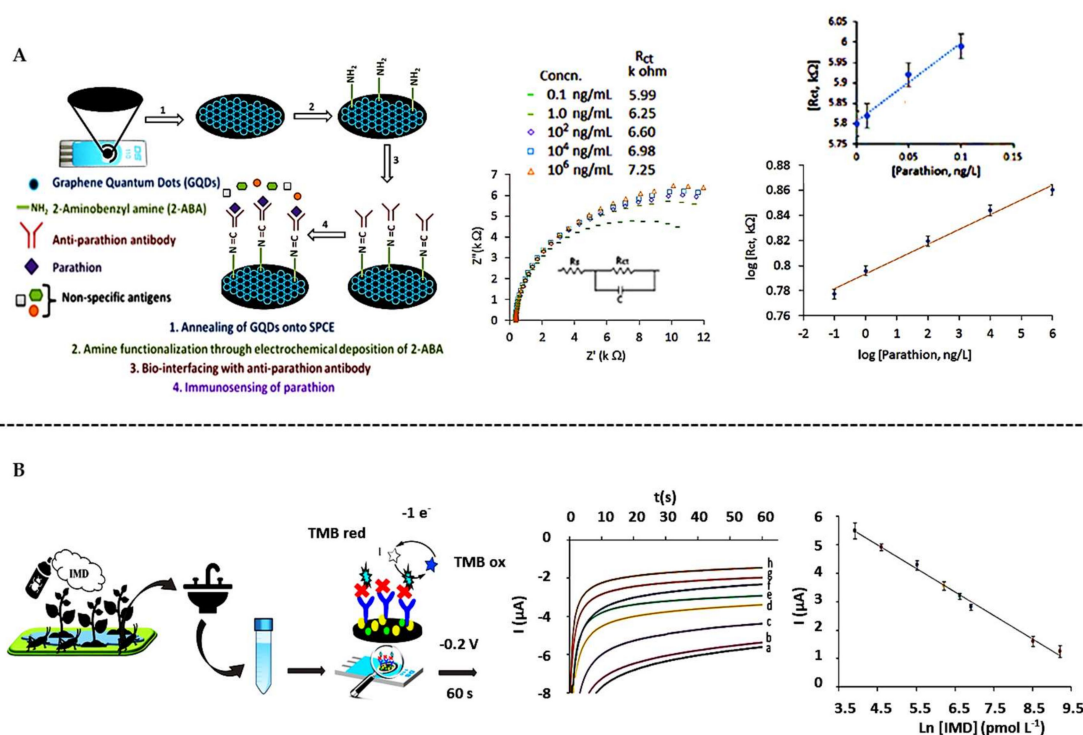


Figure 6. Immunosensors for the determination of pesticides on screen-printed electrodes. (A) Use of GQDs to determine Parathion, Nyquist curves and calibration curve. Reprinted from [177], Copyright 2017, with permission from Elsevier. (B) Direct competitive immunosensor using AuNPs for the determination of Imidacoprid (IMD), chronoamperometric measurements and calibration curve. Reprinted from [180], Copyright 2020, with permission from Elsevier.

6. Aptasensors

Aptamers are single-chain oligonucleotides that can be produced through the technique of “systematic evolution of ligands by exponential enrichment” (SELEX) [184]. These aptamers are able to fold into three-dimensional structures to bind small compounds such as pesticides and drugs or large organisms [185–190]. Aptamers and analytes are joined by Van der Waals forces, electrostatic interactions or hydrogen bonds [191], thus being able to reverse the aptamer/analyte bond. Some of the advantages of the use of aptamers are the lower cost with respect to enzymes and antibodies, higher stability, long service life, regeneration possibilities and simplicity and rapid response [185,192]. Aptamers can also be easily functionalized and immobilized on the SPE for the development of electrochemical aptasensors.

However, their use for the detection of pesticides has not been extensively reported, as shown in Table 5. Again, SPE modification with different (nano)materials seems to be crucial for improving the efficiency of both the aptamer immobilization and the electrochemical detection.

As example, polyaniline/AuNPs composites were proposed by Rapini et al. [193] for the immobilization of an acetamiprid-specific aptamer (Figure 7A). The pesticide detection was based on a competitive assay using an enzyme-tagged oligonucleotide complementary to the aptamer sequence, reaching a LOD of 86 nM with high selectivity. Good performance was also obtained when analyzing blackberry, apricot and peach juice samples.

Table 5. Aptasensors reported for pesticides determination on screen-printed electrodes.

Electrode	Analyte	Lineal range	LoD	Ref
Apt/PANI/AuNPs/SPGE	Acetamiprid	0.25–2 μ M	86 nM	[193]
BSA/Apt/rGO-CuNPs/SPCE	Profenofos	0.01–100 nM	3 pM	[194]
	Phorate	1–1000 nM	300 pM	
	Isocarbophos	0.1–1000 nM	30 pM	
	Omethoate	1–500 nM	300 pM	
Apt/MCH/AuNP/AuSPE	Diazinon	0.1–1000 nM	17 pM	[195]

Apt: Aptamer; PANI: Polyaniline layer; SPGE: Screen-printed graphite electrode; MCH: 6-Mercapto-1-hexanol; AuSPE: Screen-printed gold electrode.

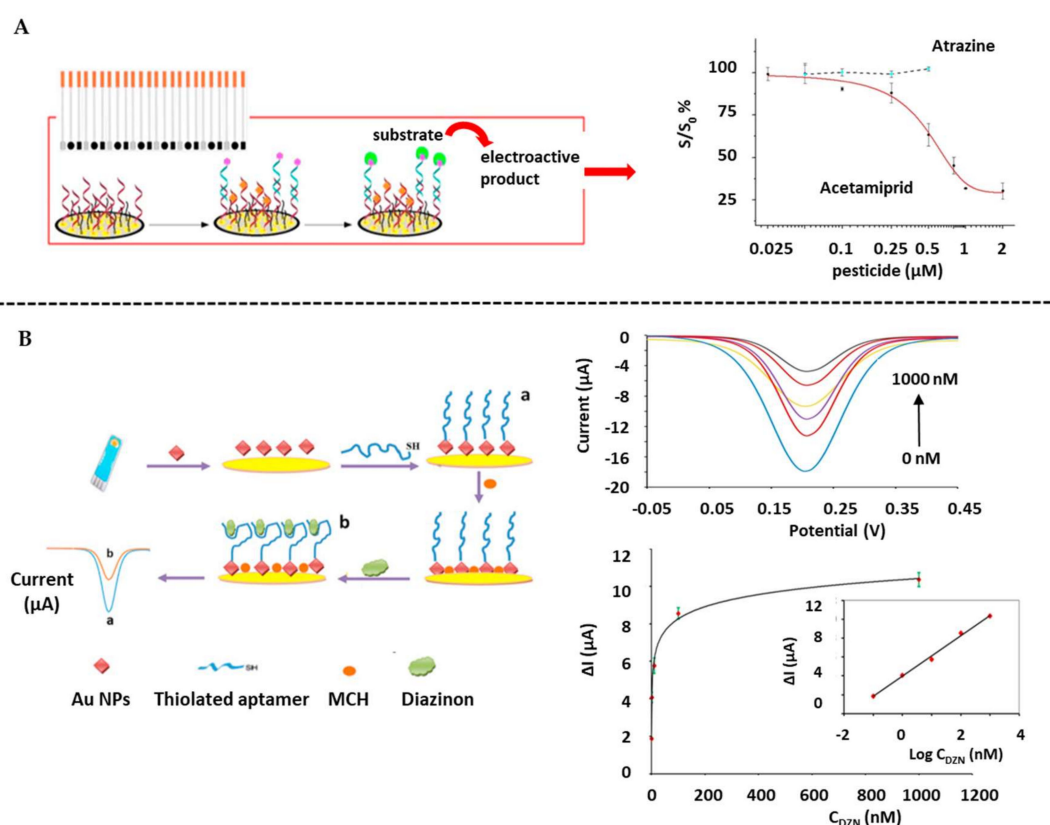


Figure 7. Aptasensors for pesticides determination on screen-printed electrodes: (A) Immobilization of aptamer on AuNPs-modified SPGE for the determination of Acetamiprid and the dose-response curve of Acetamiprid and Atrazine. Adapted from [193], Copyright 2016, with permission from Elsevier. (B) Immobilization of aptamer on AuNPs-modified gold SPE for Diazinon detection and DPV measurements at different concentrations together with the calibration curve. Reprinted from [195], Copyright 2018, with permission from Elsevier.

Aptamers have also been immobilized on SPE in composites with reduced graphene oxide (rGO) and Cu nanoparticles (CuNP). That is the case of the work reported by Fu et al. [194] for the determination of organophosphorus pesticides. The voltammetric signal decreases when increasing the pesticide concentration, since the complex aptamer-pesticide hindered the transfer electron of the $[\text{Fe}(\text{CN})_6]^{3-/4-}$ ions. Under the optimal conditions LoDs ranging from of 0.003 to 0.3 nM were obtained for Profenofos, Phorate, Isocarbophos and Omethoate. The aptasensor was also successfully applied for rapeseed and spinach samples, after an extraction treatment.

AuNP-modified SPEs were also proposed for the immobilization of an aptamer specific for Diazinon (DZN) [195]. Increase in the impedance upon pesticide recognition was approached for its

determination at levels as low as 17 fM, also taking advantage of the AuNPs as enhancers of the electronic transference (Figure 7B). Rat plasma samples were also analyzed with good sensor performance.

7. Biological Sensors

Cells and microorganisms can also be used as recognition elements in biosensors. In this case the analytical signal is commonly related to the activation or inactivation of cellular respiration upon analyte interaction, leading to the production of electroactive metabolites. A representative approach consists in the genetic modification of microorganisms with enzymes, such as OPH for the determination of organophosphorus pesticides by measuring the enzymatically produced p-nitrophenol [102,196–198].

However, a key limitation of using microorganisms as a recognition element relies in their low sensitivity and long analysis time because of the slow transport of substrate and product through the cytoplasmic membranes of the cells. Due to this, few works on the use of microorganisms for the development of pesticide biosensors on SPE are found in the literature, as summarized in Table 6. From these works, the report by Touloupakis et al. deserves to be highlighted [199] which employed Photosystem II (PS II) that has an oxidoreductase-like behavior. In this work, they used the photosynthetic thylakoid of *Spinacia oleracea*, *Senecio vulgaris* and its atrazine resistant mutant immobilized with BSA-GA on the SPE for the detection of herbicides that selectively block the electronic transfer activity of PS II biomediators (Figure 8A). The developed multi-biosensor reached LoDs at levels ranging from 15 to 41 nM for Diuron, Atrazine, Simazine, Terbutylazine and Deethylterbutylazine, even in river water samples.

Table 6. Biological sensors reported for pesticides determination on screen-printed electrodes.

Bacteria	Analyte	Lineal range	LoD	Ref
<i>Spinacia oleracea</i> <i>Senecio vulgaris</i>	DIU	1×10^{-8} – 1×10^{-6} M	15 nM	[199]
	ATR	1×10^{-8} – 1×10^{-6} M	13 nM	
	SIM	1×10^{-8} – 1×10^{-6} M	41 nM	
	TER	1×10^{-9} – 1×10^{-6} M	25 nM	
	DET	1×10^{-8} – 1×10^{-6} M	24 nM	
<i>Rhodobacter sphaeroides</i>	Terbutryn	0.001–10 μ M	8 nM	[200]
<i>Escherichia coli</i>	Methyl parathion	2–80 μ M	0.5 μ M	[201]

DIU: Diuron; ATR: Atrazine; SIM: Simazine; TER: Terbutylazine; DET: Deethylterbutylazine.

Alternatively Chatzipetrou et al. [200] used as recognition elements the bacterial reaction centers (RC) of *Rhodobacter sphaeroides* immobilized on gold SPE for the determination of Terbutryn at 8 nM levels (Figure 8B).

Finally, the biosensor reported by Kumar and D'Souza [201] is based on the immobilization of whole cells of recombinant *Escherichia coli* on an SPCE for the detection of Methyl parathion. The organophosphorus hydrolase enzyme that catalyzes the hydrolysis of organophosphorus pesticides such as Methyl parathion in p-nitrophenol is expressed in recombinant *Escherichia coli* cells, being an electroactive compound through which the concentration of Methyl parathion is directly determined. With this approach, Methyl parathion was detected at 0.5 μ M levels.

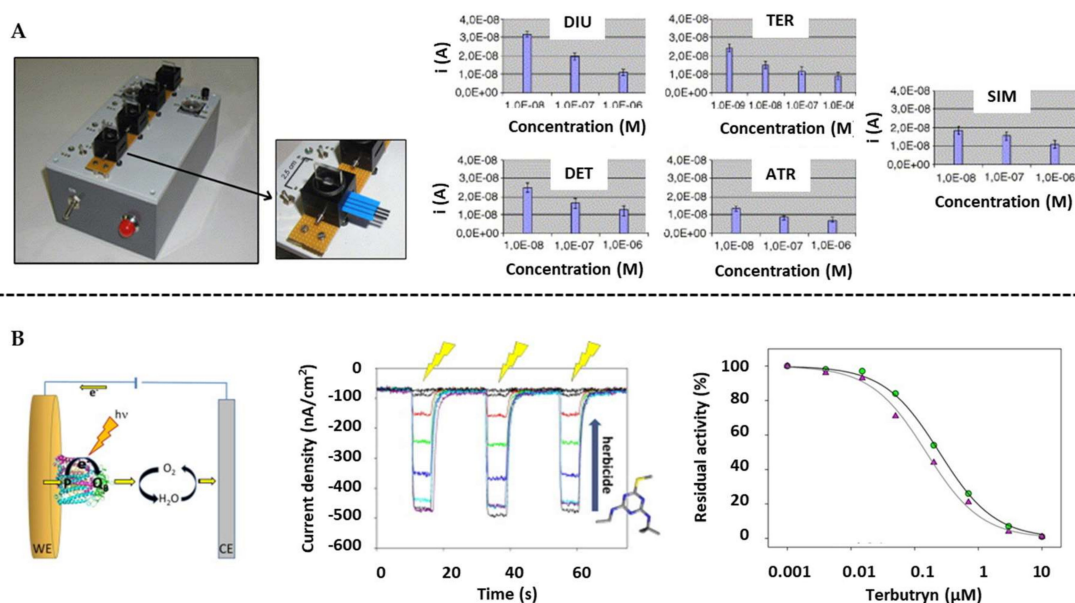


Figure 8. Biological sensors for pesticides determination on screen-printed electrodes: (A) Multi-flow detector device for the determination of herbicides using PS II as oxidoreductase. Representation of the current decrease with the herbicide's concentrations. Reprinted from [199], Copyright 2005, with permission from Elsevier. (B) Scheme of a biosensor using bacterial reaction centers on gold SPE for the determination of Terbutryn. Photocurrents detected by LIFT and Terbutryn curves in absence and presence of 80 μM of 2,3-dimethoxy-5-methyl-p-benzoquinone (UQ_0) (inset the Dixon plot). Reprinted from [200], Copyright 2016, with permission from Elsevier.

8. Conclusions

Screen-printed electrodes (SPEs) are emerging platforms with outstanding potential for their use as transducers in electrochemical (bio)sensing of pesticides. Their well-known advantages in terms of disposability, portability and low-volumes required, among others, make them ideal for the “in field” detection of pesticides at the point of need. Moreover, their versatility and easy modification with different materials is of key relevance for reaching ultralow detection limits that allow to detect the pesticides at the maximum levels allowed by the legislation. In this line, the use of nanomaterials, such as carbon-related ones (graphene, carbon nanotubes) and metallic nanoparticles is the object of an extensive research in recent years.

The (bio)sensing strategy to be followed for the pesticide detection must be carefully studied for each concrete case.

The simpler and faster strategy consists in the direct detection, taking advantage of the electroactivity of some pesticides, that is the presence of functional groups with red-ox properties. However, a limited group of pesticides can be sensitively detected through this route, typically at levels of μM – nM .

Enzymatic sensors are the most widely used, benefitting from the wide range of pesticides able to be detected and the high sensitivity reached, typically at levels of nM – pM . However, the use of enzymes entails important limitations related to their low stability over time and their sensitivity to changes in temperature and pH, among others, so alternative biosensing methods based on antibody receptors, are becoming popular in the last years.

The main advantages of such immunosensors over the enzyme-based ones rely on the higher stability of antibodies together with their superior selectivity and specificity. The detection limits reached are quite similar to the ones obtained through the enzymatic route, typically at pM levels. The high cost and low availability of monoclonal antibodies and the small size of the pesticides that

usually avoids sandwich-based approaches are important limitations that should be considered before selecting this biosensing approach.

In conclusion, the selectivity and sensitivity/detection limit required, and the availability of specific enzymes and antibodies are the main parameters that should define the detection strategy more suitable for each particular application.

As far as we know, none of the reported electrochemical (bio)sensors for pesticides detection on SPEs are commercially available yet. In this line, some important issues should be solved for the implantation of such (bio)sensing systems for routine analysis, as alternative to centralized laboratory-based methods (HPLC-MS/MS; GC-MS/MS). Efficiency and long-term stability of the enzymes and the antibodies are crucial issues that are not addressed in most of the reviewed works. Moreover, multi-detection abilities should be strongly required for real applications in pesticides screening. Efforts in this sense should be the next at the current state of the art.

Overall, the higher potentiality of SPE-based pesticide (bio)sensors is in the decentralized “in field” analysis, in our opinion. The combination of such miniaturized electrochemical transducers, the cheap and portable electrochemical instruments and the stability of mainly the antibodies make altogether ideal for such applications. In the case of the immunosensors, the most challenging issue is related to the sampling, washing, etc. steps required, which limits their use by non-skilled people and consequently their commercial implantation. The combination with microfluidics seems to be of key relevance here, so high efforts in this sense are previewed for the coming years.

Author Contributions: B.P.-F.; writing—review and editing, A.C.-G.; funding acquisition, A.d.I.E.-M.; writing—review and editing and funding acquisition. All authors have read and agreed to the published version of the manuscript.

Funding: This research was funded by FC-GRUPIN-ID/2018/000166 project from the Asturias Regional Government and the CTQ2017-86994-R project from the Spanish Ministry Economy and Competitiveness (MINECO). A. de la Escosura-Muñiz acknowledges the Spanish Ministry of Science, Innovation and Universities (MICINN) for the “Ramón y Cajal” Research Fellow (RyC-2016-20299).

Conflicts of Interest: The authors declare no conflict of interest.

References

1. World Health Organization. *Human Biomonitoring: Facts and Figures*; WHO Regional Office for Europe: Copenhagen, Denmark, 2015.
2. WHO (World Health Organization). Available online: <https://www.who.int/> (accessed on 30 December 2019).
3. United States Environmental Protection Agency (US EPA). Available online: <https://www.epa.gov/> (accessed on 30 December 2019).
4. Consejo de la Unión Europea Directiva 98/83/CE del Consejo. *Off. J. Eur. Communities* **1998**, *L330*, 32–54.
5. Caso, E.L.; Plaguicidas, C.D.E.L.O.S. Análisis de la directiva europea 98/83/CE: Paradigma de la justificación y establecimiento de los valores paramétricos. *El caso concreto de los plaguicidas*. **2012**, *86*, 21–35.
6. Oficial, D.; Comisi, D.E.L.A.; Europeo, P.; Europeo, P.; Alimentarius, C. Scientific support for preparing an EU position for the 45th Session of the Codex Committee on Pesticide Residues (CCPR). *EFSA J.* **2013**, *11*, 1–5.
7. Human Resources Council. United Nations General Assembly. *Report of the Special Rapporteur on the Right to food*. Available online: <https://www.ohchr.org/en/issues/food/pages/foodindex.aspx> (accessed on 30 December 2019).
8. Anagnostopoulos, C.; Miliadis, G.E. Development and validation of an easy multiresidue method for the determination of multiclass pesticide residues using GC-MS/MS and LC-MS/MS in olive oil and olives. *Talanta* **2013**, *112*, 1–10. [[CrossRef](#)] [[PubMed](#)]
9. Xiao, Z.; Yang, Y.; Li, Y.; Fan, X.; Ding, S. Determination of neonicotinoid insecticides residues in eels using subcritical water extraction and ultra-performance liquid chromatography-tandem mass spectrometry. *Anal. Chim. Acta* **2013**, *777*, 32–40. [[CrossRef](#)] [[PubMed](#)]
10. Huang, Y.; Shi, T.; Luo, X.; Xiong, H.; Min, F.; Chen, Y. Determination of multi-pesticide residues in green tea with a modified QuEChERS protocol coupled to HPLC-MS/MS. *Food Chem.* **2019**, *275*, 255–264. [[CrossRef](#)] [[PubMed](#)]

11. Timofeeva, I.; Shishov, A.; Kanashina, D.; Dzema, D.; Bulatov, A. On-line in-syringe sugaring-out liquid-liquid extraction coupled with HPLC-MS/MS for the determination of pesticides in fruit and berry juices. *Talanta* **2017**, *167*, 761–767. [[CrossRef](#)] [[PubMed](#)]
12. Song, N.; Lee, J.Y.; Mansur, A.R.; Jang, H.W.; Lim, M.; Lee, Y. Determination of 60 pesticides in hen eggs using the QuEChERS procedure followed by LC-MS/MS and GC-MS/MS. *Food Chem.* **2019**, *298*, 125050. [[CrossRef](#)]
13. Zhu, B.; Xu, X.; Luo, J.; Jin, S.; Chen, W.; Liu, Z. Simultaneous determination of 131 pesticides in tea by on-line GPC-GC – MS/MS using graphitized multi-walled carbon nanotubes as dispersive solid phase extraction sorbent. *Food Chem.* **2019**, *276*, 202–208. [[CrossRef](#)]
14. Li, M.; Li, D.; Xiu, G.; Long, Y. Applications of screen-printed electrodes in current environmental analysis. *Curr. Opin. Electrochem.* **2012**, *3*, 137–143. [[CrossRef](#)]
15. Mullane, A.P.O. Electrochemistry. *Ref. Modul. Chem. Mol. Sci. Chem. Eng.* **2013**, *2*, 1–3.
16. Oja, S.M.; Wood, M.; Zhang, B. Nanoscale electrochemistry. *Anal. Chem.* **2013**, *85*, 473–486. [[CrossRef](#)] [[PubMed](#)]
17. Renedo, O.D.; Alonso-Lomillo, M.A.; Martínez, M.J.A. Recent developments in the field of screen-printed electrodes and their related applications. *Talanta* **2007**, *73*, 202–219. [[CrossRef](#)] [[PubMed](#)]
18. Fanjul-Bolado, P.; Hernández-Santos, D.; Lamas-Ardisana, P.J.; Martín-Pernía, A.; Costa-García, A. Electrochemical characterization of screen-printed and conventional carbon paste electrodes. *Electrochim. Acta* **2008**, *53*, 3635–3642. [[CrossRef](#)]
19. Lebig-elhadi, H.; Frontistis, Z.; Ait-amar, H.; Amrani, S. Electrochemical oxidation of pesticide thiamethoxam on boron doped diamond anode: Role of operating parameters and matrix effect. *Process Saf. Environ. Prot.* **2018**, *116*, 535–541. [[CrossRef](#)]
20. Chorti, P.; Fischer, J.; Vyskocil, V.; Economou, A.; Barek, J. Electrochimica Acta Voltammetric Determination of Insecticide Thiamethoxam on Silver Solid Amalgam Electrode. *Electrochim. Acta* **2014**, *140*, 5–10. [[CrossRef](#)]
21. Chu, Z.; Peng, J.; Jin, W. Advanced nanomaterial inks for screen-printed chemical sensors. *Sens. Actuators B Chem.* **2017**, *243*, 919–926. [[CrossRef](#)]
22. Martín-Yerga, D.; Costa Rama, E.; Costa García, A.A. Electrochemical study and determination of electroactive species with screen-printed electrodes. *J. Chem. Educ.* **2016**, *93*, 1270–1276. [[CrossRef](#)]
23. Arduini, F.; Micheli, L.; Moscone, D.; Palleschi, G.; Piermarini, S.; Ricci, F.; Volpe, G. Electrochemical biosensors based on nanomodified screen-printed electrodes: Recent applications in clinical analysis. *Trends Anal. Chem.* **2016**, *79*, 114–126. [[CrossRef](#)]
24. Fahem, D.K.; El, O.M.; El-rahman, M.K.A.; Zaazaa, H.E. A point of care screen printed potentiometric sensor for therapeutic monitoring of vecuronium. *Microchem. J.* **2019**, *147*, 532–537. [[CrossRef](#)]
25. Garcia, P.T.; Guimarães, L.N.; Dias, A.A.; Ulhoa, C.J.; Coltro, W.K.T. Amperometric detection of salivary α -amylase on screen-printed carbon electrodes as a simple and inexpensive alternative for point-of-care testing. *Sens. Actuators B Chem.* **2018**, *258*, 342–348. [[CrossRef](#)]
26. Moreira, F.T.C.; Dutra, R.A.F.; Noronha, J.P.C.; Fernandes, J.C.S.; Sales, M.G.F. Novel biosensing device for point-of-care applications with plastic antibodies grown on Au-screen printed electrodes. *Sens. Actuators B Chem.* **2013**, *182*, 733–740. [[CrossRef](#)]
27. Kampeera, J.; Pasakon, P.; Karuwan, C.; Arunrut, N. Point-of-care rapid detection of *Vibrio parahaemolyticus* in seafood using loop-mediated isothermal amplification and graphene-based screen-printed electrochemical sensor. *Biosens. Bioelectron.* **2019**, *132*, 271–278. [[CrossRef](#)] [[PubMed](#)]
28. Pérez-Fernández, B.; Martín-Yerga, D.; Costa-García, A. Electrodeposition of nickel nanoflowers on screen-printed electrodes and its application to non-enzymatic determination of sugars. *RSC Adv.* **2016**, *6*, 83748–83757. [[CrossRef](#)]
29. Pérez-Fernández, B.; Martín-Yerga, D.; Costa-García, A. Galvanostatic electrodeposition of copper nanoparticles on screen-printed carbon electrodes and their application for reducing sugars determination. *Talanta* **2017**, *175*, 108–113. [[CrossRef](#)] [[PubMed](#)]
30. Martínez-Paredes, G.; González-García, M.B.; Costa-García, A. In situ electrochemical generation of gold nanostructured screen-printed carbon electrodes. Application to the detection of lead underpotential deposition. *Electrochim. Acta* **2009**, *54*, 4801–4808. [[CrossRef](#)]
31. Kardaş, F.; Beytur, M.; Akyıldırım, O.; Yüksek, H.; Yola, M.L.; Atar, N. Electrochemical detection of atrazine in wastewater samples by copper oxide (CuO) nanoparticles ionic liquid modified electrode. *J. Mol. Liq.* **2017**, *248*, 360–363. [[CrossRef](#)]

32. Zhao, H.; Zhou, C.; Teng, Y.; Chen, C.; Lan, M. Applied Surface Science Novel Pt nanowires modified screen-printed gold electrode by electrodeposited method. *Appl. Surf. Sci.* **2011**, *257*, 3793–3797. [[CrossRef](#)]
33. Youse, A.; Babaei, A.; Delavar, M. Application of modified screen-printed carbon electrode with MWCNTs-Pt-doped CdS nanocomposite as a sensitive sensor for determination of natamycin in yoghurt drink and cheese. *J. Electroanal. Chem.* **2018**, *822*, 1–9. [[CrossRef](#)]
34. Song, Y.; Chen, J.; Sun, M.; Gong, C.; Shen, Y.; Song, Y.; Wang, L. A simple electrochemical biosensor based on AuNPs / MPS / Au electrode sensing layer for monitoring carbamate pesticides in real samples. *J. Hazard. Mater.* **2016**, *304*, 103–109. [[CrossRef](#)]
35. Tajik, S.; Safaei, M.; Beitollahi, H. A sensitive voltammetric sertraline nanosensor based on ZnFe₂O₄ nanoparticles modified screen printed electrode. *Measurement* **2019**, *143*, 51–57. [[CrossRef](#)]
36. Zia, S.; Beitollahi, H.; Allahabadi, H.; Rohani, T. Disposable electrochemical sensor based on modified screen printed electrode for sensitive cabergoline quantification. *J. Electroanal. Chem.* **2019**, *847*, 113223.
37. Chen, Y.; Kirankumar, R.; Kao, C.; Chen, P. Electrodeposited Ag, Au, and AuAg nanoparticles on graphene oxide-modified screen-printed carbon electrodes for the voltammetric determination of free sulfide in alkaline solutions. *Electrochim. Acta* **2016**, *205*, 124–131. [[CrossRef](#)]
38. Jeromiyas, N.; Elaiyappillai, E.; Senthil, A. Bismuth nanoparticles decorated graphenated carbon nanotubes modified screen-printed electrode for mercury detection. *J. Taiwan Inst. Chem. Eng.* **2019**, *95*, 466–474. [[CrossRef](#)]
39. Xuan, N.; Xuan, N.; Takamura, Y. Development of highly sensitive electrochemical immunosensor based on single-walled carbon nanotube modified screen-printed carbon electrode. *Mater. Chem. Phys.* **2019**, *227*, 123–129.
40. Tpra, R. Electrochemiluminescence study of AuNPs/CdTe-QDs/SWCNTs/chitosan nanocomposite modified carbon nanofiber screen-printed electrode with [Ru(bpy)₃]²⁺/TPrA. *Inorg. Chem. Commun.* **2019**, *106*, 54–60.
41. Singh, M.; Tiwari, I.; Foster, C.W.; Banks, C.E. Highly sensitive and selective determination of dopamine using screen- printed electrodes modified with nanocomposite of N'-phenyl-p-phenylenediamine/multiwalled carbon nanotubes/nafion. *Mater. Res. Bull.* **2018**, *101*, 253–263. [[CrossRef](#)]
42. Lamas-Ardisana, P.A.; Queipo, P.; Fanjul-Bolado, P.; Costa-garcia, A. Multiwalled carbon nanotube modified screen-printed electrodes for the detection of p -aminophenol: Optimisation and application in alkaline phosphatase-based assays. *Anal. Chim. Acta* **2008**, *615*, 30–38. [[CrossRef](#)]
43. García-González, R.; Fernández-Abedul, M.T.; Costa-García, A. Nafion modified-screen printed gold electrodes and their carbon nanostructuring for electrochemical sensors applications. *Talanta* **2013**, *107*, 376–381. [[CrossRef](#)]
44. Calder, J.A.; Nagles, E.; García-beltr, O. Evaluation of the usefulness of a novel electrochemical sensor in detecting uric acid and dopamine in the presence of ascorbic acid using a screen-printed carbon electrode modified with single walled carbon nanotubes and ionic liquids. *Electrochim. Acta* **2017**, *258*, 512–523.
45. Gutiérrez, C.; Squella, J.A. Carbon nanofiber screen printed electrode joined to a flow injection system for nimodipine sensing. *Sens. Actuators B Chem.* **2015**, *220*, 456–462.
46. Nellaiappan, S.; Senthil, A. Electrocatalytic oxidation and flow injection analysis of isoniazid drug using a gold nanoparticles decorated carbon nanofibers-chitosan modified carbon screen printed electrode in neutral pH. *J. Electroanal. Chem.* **2017**, *801*, 171–178. [[CrossRef](#)]
47. Pérez-ràfols, C.; Serrano, N.; Díaz-cruz, J.M.; Ariño, C.; Esteban, M. Glutathione modified screen-printed carbon nanofiber electrode for the voltammetric determination of metal ions in natural samples. *Talanta* **2016**, *155*, 8–13. [[CrossRef](#)] [[PubMed](#)]
48. Lamas-ardisana, P.J.; Fanjul-bolado, P.; Costa-garcía, A. Manufacture and evaluation of cup-stacked carbon nanofiber-modified screen printed electrodes as electrochemical tools. *JEAC* **2016**, *775*, 129–134. [[CrossRef](#)]
49. Samie, H.A.; Arvand, M. RuO₂ nanowires on electrospun CeO₂ -Au nanofibers/functionalized carbon nanotubes / graphite oxide nanocomposite modified screen-printed carbon electrode for simultaneous determination of serotonin, dopamine and ascorbic acid. *J. Alloys Compd.* **2019**, *782*, 824–836. [[CrossRef](#)]
50. Chan, K.F.; Lim, H.N.; Shams, N.; Jayabal, S.; Pandikumar, A.; Huang, N.M. Fabrication of graphene / gold-modified screen-printed electrode for detection of carcinoembryonic antigen. *Mater. Sci. Eng. C* **2016**, *58*, 666–674. [[CrossRef](#)]

51. Sánchez Calvo, A.; Botas, C.; Martín-Yerga, D.; Álvarez, P.; Menéndez, R.; Costa-García, A. Comparative Study of Screen-Printed Electrodes Modified with Graphene Oxides Reduced by a Constant Current. *J. Electrochem. Soc.* **2015**, *162*, B282–B290. [[CrossRef](#)]
52. Jaiswal, N.; Tiwari, I.; Foster, C.W.; Banks, C.E. Highly sensitive amperometric sensing of nitrite utilizing bulk-modified MnO₂ decorated Graphene oxide nanocomposite screen-printed electrodes. *Electrochim. Acta* **2017**, *227*, 255–266. [[CrossRef](#)]
53. Thunkhamrak, C.; Chuntib, P.; Ounnunkad, K.; Banet, P. Highly sensitive voltammetric immunosensor for the detection of prostate specific antigen based on silver nanoprobe assisted graphene oxide modified screen printed carbon electrode. *Talanta* **2020**, *208*, 120389. [[CrossRef](#)]
54. Li, S.; Zhang, Q.; Lu, Y.; Ji, D.; Zhang, D.; Wu, J.; Chen, X.; Liu, Q. One step electrochemical deposition and reduction of graphene oxide on screen printed electrodes for impedance detection of glucose. *Sens. Actuators B Chem.* **2017**, *244*, 290–298. [[CrossRef](#)]
55. Singh, M.; Jaiswal, N.; Tiwari, I.; Foster, C.W.; Banks, C.E. A reduced graphene oxide-cyclodextrin-platinum nanocomposite modified screen printed electrode for the detection of cysteine. *J. Electroanal. Chem.* **2018**, *829*, 230–240. [[CrossRef](#)]
56. Maity, D.; Minitha, C.R.; Rajendra Kumar, R.T. Glucose oxidase immobilized amine terminated multiwall carbon nanotubes/reduced graphene oxide/polyaniline/gold nanoparticles modified screen-printed carbon electrode for highly sensitive amperometric glucose detection. *Mater. Sci. Eng. C* **2019**, *105*, 110075. [[CrossRef](#)] [[PubMed](#)]
57. Ibáñez-Redín, G.; Wilson, D.; Gonçalves, D.; Oliveira, O.N., Jr. Low-cost screen-printed electrodes based on electrochemically reduced graphene oxide-carbon black nanocomposites for dopamine, epinephrine and paracetamol detection. *J. Colloid Interface Sci.* **2018**, *515*, 101–108. [[CrossRef](#)] [[PubMed](#)]
58. Wang, Y.; Huang, B.; Dai, W.; Ye, J.; Xu, B. Sensitive determination of capsaicin on Ag / Ag₂O nanoparticles / reduced graphene oxide modified screen-printed electrode. *JEAC* **2016**, *776*, 93–100. [[CrossRef](#)]
59. Martín-Yerga, D.; Costa-García, A. Stabilization of electrogenerated copper species at quantum dots-modified electrodes. *Phys. Chem. Chem. Phys.* **2017**, *74*, 53–56.
60. Kokkinos, C.; Prodromidis, M.; Economou, A.; Petrou, P. Disposable integrated bismuth citrate-modified screen-printed immunosensor for ultrasensitive quantum dot-based electrochemical assay of C-reactive protein in human serum. *Anal. Chim. Acta* **2015**, *886*, 29–36. [[CrossRef](#)]
61. Martín-yerga, D.; González-garcía, M.B.; Costa-garcía, A. Electrochemical immunosensor for anti-tissue transglutaminase antibodies based on the in situ detection of quantum dots. *Talanta* **2014**, *130*, 598–602. [[CrossRef](#)]
62. García, C.; Navarro, F.; Celis, F.; Ruiz, D.; Toledo, S.; Sanhueza, L.; Qui, A. Electrochemical, spectroscopic and electrochemiluminescent characterization of self-assembled 3-aminopropyltriethoxysilane/CdTe quantum dots hybrids on screen-printed electrodes. *Electrochim. Acta* **2018**, *276*, 64–72. [[CrossRef](#)]
63. Roushani, M.; Jalilian, Z.; Nezhadali, A. Screen printed carbon electrode sensor with thiol graphene quantum dots and gold nanoparticles for voltammetric determination of solatol. *Heliyon* **2019**, *5*, e01984. [[CrossRef](#)]
64. Campuzano, S.; Paloma, Y.; Asadpour-zeynali, K. Ultrasensitive determination of receptor tyrosine kinase with a label-free electrochemical immunosensor using graphene quantum dots- modified screen-printed electrodes. *Anal. Chim. Acta* **2018**, *1011*, 28–34.
65. Centi, S.; Laschi, S.; Fr, M.; Mascini, M. A disposable immunomagnetic electrochemical sensor based on functionalised magnetic beads and carbon-based screen-printed electrodes (SPCEs) for the detection of polychlorinated biphenyls (PCBs). *Anal. Chim. Acta* **2005**, *538*, 205–212. [[CrossRef](#)]
66. Eguílaz, M.; Moreno-guzmán, M.; Campuzano, S.; González-cortés, A.; Pingarrón, J.M.; Yá, P. An electrochemical immunosensor for testosterone using functionalized magnetic beads and screen-printed carbon electrodes. *Biosens. Bioelectron.* **2010**, *26*, 517–522. [[CrossRef](#)] [[PubMed](#)]
67. Biscay, J.; Begoña, M.; García, G.; Costa, A. Electrochemical biotin detection based on magnetic beads and a new magnetic flow cell for screen printed electrode. *Talanta* **2015**, *131*, 706–711. [[CrossRef](#)] [[PubMed](#)]
68. Biscay, J.; García, M.B.G.; García, A.C. Electrochemical biotin determination based on a screen printed carbon electrode array and magnetic beads. *Sens. Actuators B Chem.* **2014**, *205*, 426–432. [[CrossRef](#)]
69. Panraksa, Y.; Siangproh, W.; Khampieng, T.; Chailapakul, O.; Apilux, A. Paper-based amperometric sensor for determination of acetylcholinesterase using screen-printed graphene electrode. *Talanta* **2018**, *178*, 1017–1023. [[CrossRef](#)]

70. Biscay, J.; Rama, E.C.; García, M.B.G.; Carrazón, J.M.P.; García, A.C. Enzymatic sensor using mediator-screen-printed carbon electrodes. *Electroanalysis* **2011**, *23*, 209–214. [[CrossRef](#)]
71. Wang, J.; Nascimento, V.B.; Kane, S.A.; Rogers, K.; Smyth, M.R.; Angnes, L. Screen-printed tyrosinase-containing electrodes for the biosensing of enzyme inhibitors. *Talanta* **1996**, *43*, 1903–1907. [[CrossRef](#)]
72. Alonso-lomillo, M.A.; Domínguez-renedo, O. Sensitive enzyme-biosensor based on screen-printed electrodes for Ochratoxin A. *Biosens. Bioelectron.* **2010**, *25*, 1333–1337. [[CrossRef](#)]
73. Alvarado-gámez, A.L.; Alonso-lomillo, M.A.; Domínguez-renedo, O.; Arcos-martínez, M.J. Vanadium determination in water using alkaline phosphatase based screen-printed carbon electrodes modified with gold nanoparticles. *J. Electroanal. Chem.* **2013**, *693*, 51–55. [[CrossRef](#)]
74. Biscay, J.; Costa Rama, E.; González García, M.B.; Julio Reviejo, A.; Pingarrón Carrazón, J.M.; García, A.C. Amperometric fructose sensor based on ferrocyanide modified screen-printed carbon electrode. *Talanta* **2012**, *88*, 432–438. [[CrossRef](#)]
75. Karim, N.; Jin, H. Amperometric phenol biosensor based on covalent immobilization of tyrosinase on Au nanoparticle modified screen printed carbon electrodes. *Talanta* **2013**, *116*, 991–996. [[CrossRef](#)] [[PubMed](#)]
76. Soln, R.; Ruzgas, T.; Skl, P. Amperometric screen-printed biosensor arrays with co-immobilised oxidoreductases and cholinesterases. *Anal. Chim. Acta* **2005**, *528*, 9–19. [[CrossRef](#)]
77. Sapelniko, S.; Dock, E.; Ruzgas, T.; Emne, J. Amperometric sensors based on tyrosinase-modified screen-printed arrays. *Talanta* **2003**, *61*, 473–483. [[CrossRef](#)]
78. Hatada, M.; Tsugawa, W.; Kamio, E.; Loew, N.; Klonoff, D.C. Development of a screen-printed carbon electrode based disposable enzyme sensor strip for the measurement of glycated albumin. *Biosens. Bioelectron.* **2017**, *88*, 167–173. [[CrossRef](#)]
79. Cerrato-alvarez, M.; Bernalte, E.; Bernalte-garcía, M.J.; Pinilla-gil, E. Fast and direct amperometric analysis of polyphenols in beers using tyrosinase-modified screen-printed gold nanoparticles biosensors. *Talanta* **2019**, *193*, 93–99. [[CrossRef](#)]
80. Dontsova, E.A.; Zeifman, Y.S.; Budashov, I.A.; Eremenko, A.V.; Kalnov, S.L.; Kurochkin, I.N. Screen-printed carbon electrode for choline based on MnO₂ nanoparticles and choline oxidase/polyelectrolyte layers. *Sens. Actuators B Chem.* **2011**, *159*, 261–270. [[CrossRef](#)]
81. Yan, M.; Zang, D.; Ge, S.; Ge, L.; Yu, J. A disposable electrochemical immunosensor based on carbon screen-printed electrodes for the detection of prostate specific antigen. *Biosens. Bioelectron.* **2012**, *38*, 355–361. [[CrossRef](#)]
82. Goud, K.Y.; Kumar, V.S.; Hayat, A.; Gobi, K.V.; Song, H.; Kim, K.; Louis, J. A highly sensitive electrochemical immunosensor for zearalenone using screen-printed disposable electrodes. *J. Electroanal. Chem.* **2019**, *832*, 336–342. [[CrossRef](#)]
83. Hern, D. Development of an immunosensor for the determination of rabbit IgG using streptavidin modified screen-printed carbon electrodes. *Talanta* **2005**, *65*, 565–573.
84. Deepthy, S.; Layek, K.; Mukherjee, R.; Kumar, K.; Ghosh, M. Development of screen-printed electrode based immunosensor for the detection of HER2 antigen in human serum samples. *Bioelectrochemistry* **2017**, *118*, 25–30.
85. Jampasa, S.; Siangproh, W.; Laocharoensuk, R.; Vilaivan, T. Electrochemical detection of c-reactive protein based on anthraquinone- labeled antibody using a screen-printed graphene electrode. *Talanta* **2018**, *183*, 311–319. [[CrossRef](#)] [[PubMed](#)]
86. Baradoke, A.; Jose, B.; Pauliukaite, R.; Forster, R.J. Properties of Anti-CA125 antibody layers on screen-printed carbon electrodes modified by gold and platinum nanostructures. *Electrochim. Acta* **2019**, *306*, 299–306. [[CrossRef](#)]
87. Ibáñez-redín, G.; Furuta, R.H.M.; Wilson, D.; Shimizu, F.M.; Materon, E.M.; Maria, L.; Batista, R.; Melendez, M.E.; Carvalho, A.L.; Manuel, R.; et al. Screen-printed interdigitated electrodes modified with nanostructured carbon nano-onion films for detecting the cancer biomarker CA19-9. *Mater. Sci. Eng. C* **2019**, *99*, 1502–1508. [[CrossRef](#)] [[PubMed](#)]
88. Eissa, S. A comparison of the performance of voltammetric aptasensors for glycated haemoglobin on different carbon nanomaterials-modified screen printed electrodes. *Mater. Sci. Eng. C* **2019**, *101*, 423–430. [[CrossRef](#)]
89. Erdem, A.; Congur, G.; Mayer, G. Aptasensor platform based on carbon nanofibers enriched screen printed electrodes for impedimetric detection of thrombin. *JEAC* **2015**, *758*, 12–19. [[CrossRef](#)]

90. Xie, D.; Li, C.; Shangguan, L.; Qi, H.; Xue, D.; Gao, Q. Click chemistry-assisted self-assembly of DNA aptamer on gold nanoparticles-modified screen-printed carbon electrodes for label-free electrochemical aptasensor. *Sens. Actuators B Chem.* **2014**, *192*, 558–564. [[CrossRef](#)]
91. Hashkavayi, A.B.; Raouf, J.B. Design an aptasensor based on structure-switching aptamer on dendritic gold nanostructures/Fe₃O₄@SiO₂/DABCO modified screen printed electrode for highly selective detection of epirubicin. *Biosens. Bioelectron.* **2017**, *91*, 650–657. [[CrossRef](#)]
92. Yeh, F.; Liu, T.; Tseng, I.; Yang, C.; Lu, L.; Lin, C. Gold nanoparticles conjugates-amplified aptamer immunosensing screen-printed carbon electrode strips for thrombin detection. *Biosens. Bioelectron.* **2014**, *61*, 336–343. [[CrossRef](#)]
93. Jo, H.; Her, J.; Lee, H.; Shim, Y.; Ban, C. Highly sensitive amperometric detection of cardiac troponin I using sandwich aptamers and screen-printed carbon electrodes. *Talanta* **2017**, *165*, 442–448. [[CrossRef](#)]
94. Ren, R.; Leng, C.; Zhang, S. A chronocoulometric DNA sensor based on screen-printed electrode doped with ionic liquid and polyaniline nanotubes. *Biosens. Bioelectron.* **2010**, *25*, 2089–2094. [[CrossRef](#)]
95. Evtugyn, G.; Mingaleva, A.; Budnikov, H.; Stoikova, E.; Vinter, V.; Eremin, S. Affinity biosensors based on disposable screen-printed electrodes modified with DNA. *Anal. Chim. Acta* **2003**, *479*, 125–134. [[CrossRef](#)]
96. Malecka, K.; Stachyra, A.; Góra-sochacka, A.; Sirko, A.; Zagórski-ostoja, W.; Radecka, H.; Radecki, J. Electrochemical genosensor based on disc and screen printed gold electrodes for detection of specific DNA and RNA sequences derived from Avian Influenza Virus H5N1. *Sens. Actuators B Chem.* **2016**, *224*, 290–297. [[CrossRef](#)]
97. Khairy, M.; Khorshed, A.A.; Rashwan, F.A.; Salah, G.A.; Abdel-wadood, H.M.; Banks, C.E. Sensitive determination of amlodipine besylate using bare/unmodified and DNA-modified screen-printed electrodes in tablets and biological fluids. *Sens. Actuators B Chem.* **2017**, *239*, 768–775. [[CrossRef](#)]
98. Zhang, Y.; Geng, X.; Ai, J.; Gao, Q.; Qi, H. Signal amplification detection of DNA using a sensor fabricated by one-step covalent immobilization of amino-terminated probe DNA onto the polydopamine-modified screen-printed carbon electrode. *Sens. Actuators B Chem.* **2015**, *221*, 1535–1541. [[CrossRef](#)]
99. Jiang, D.; Liu, Y.; Jiang, H.; Rao, S.; Fang, W.; Wu, M.; Yuan, L. A novel screen-printed mast cell-based electrochemical sensor for detecting spoilage bacterial quorum signaling molecules (N-acyl-homoserine-lactones) in freshwater fish. *Biosens. Bioelectron.* **2018**, *102*, 396–402. [[CrossRef](#)]
100. Chang, J.; Lien, C.; Vijayakumar, P.S.; Hsieh, P.; Zen, J. Electrochemical regulation of microbial growth on disposable screen printed carbon electrodes. *Electrochim. Acta* **2012**, *82*, 103–108. [[CrossRef](#)]
101. Wen, J.; He, D.; Yu, Z.; Zhou, S. In situ detection of microbial c-type cytochrome based on intrinsic peroxidase-like activity using screen-printed carbon electrode. *Biosens. Bioelectron.* **2018**, *113*, 52–57. [[CrossRef](#)]
102. Mulchandani, A.; Rajesh. Microbial biosensors for organophosphate pesticides. *Appl. Biochem. Biotechnol.* **2011**, *165*, 687–699. [[CrossRef](#)]
103. Kurbanoglu, S.; Ozkan, S.A.; Merkoçi, A. Nanomaterials-based enzyme electrochemical biosensors operating through inhibition for biosensing applications. *Biosens. Bioelectron.* **2017**, *89*, 886–898. [[CrossRef](#)]
104. Dou, J.; Fan, F.; Ding, A.; Cheng, L.; Sekar, R.; Wang, H.; Li, S. A screen-printed, amperometric biosensor for the determination of organophosphorus pesticides in water samples. *J. Environ. Sci.* **2012**, *24*, 956–962. [[CrossRef](#)]
105. Arduini, F.; Ricci, F.; Tuta, C.S.; Moscone, D.; Amine, A.; Palleschi, G. Detection of carbamic and organophosphorous pesticides in water samples using a cholinesterase biosensor based on Prussian Blue-modified screen-printed electrode. *Anal. Chim. Acta* **2006**, *580*, 155–162. [[CrossRef](#)] [[PubMed](#)]
106. Istamboulie, G.; Sikora, T.; Jubete, E.; Ochoteco, E.; Marty, J.; Noguer, T. Screen-printed poly (3, 4-ethylenedioxythiophene) (PEDOT): A new electrochemical mediator for acetylcholinesterase-based biosensors. *Talanta* **2010**, *82*, 957–961. [[CrossRef](#)] [[PubMed](#)]
107. Silva, G.; Jeanty, G.; Marty, J. Enzyme immobilization procedures on screen-printed electrodes used for the detection of anticholinesterase pesticides Comparative study. *Anal. Chim. Acta* **2004**, *523*, 107–115. [[CrossRef](#)]
108. Ivanov, A.N.; Younusov, R.R.; Evtugyn, G.A.; Arduini, F.; Moscone, D.; Palleschi, G. Acetylcholinesterase biosensor based on single-walled carbon nanotubes—Co phtalocyanine for organophosphorus pesticides detection. *Talanta* **2011**, *85*, 216–221. [[CrossRef](#)] [[PubMed](#)]
109. Haddaoui, M.; Raouafi, N. Chlortoluron-induced enzymatic activity inhibition in tyrosinase/ZnO NPs/SPCE biosensor for the detection of ppb levels of herbicide. *Sens. Actuators B Chem.* **2015**, *219*, 171–178. [[CrossRef](#)]

110. Wang, H.; Zhao, G.; Chen, D.; Wang, Z.; Liu, G. A sensitive acetylcholinesterase biosensor based on screen printed electrode modified with Fe₃O₄ nanoparticle and graphene for chlorpyrifos determination. *Int. J. Electrochem. Sci.* **2016**, *11*, 10906–10918. [[CrossRef](#)]
111. Shi, M.; Xu, J.; Zhang, S.; Liu, B.; Kong, J. A mediator-free screen-printed amperometric biosensor for screening of organophosphorus pesticides with flow-injection analysis (FIA) system. *Talanta* **2006**, *68*, 1089–1095. [[CrossRef](#)]
112. Cinti, S.; Neagu, D.; Carbone, M.; Cacciotti, I.; Moscone, D.; Arduini, F. Novel carbon black-cobalt phthalocyanine nanocomposite as sensing platform to detect organophosphorus pollutants at screen-printed electrode. *Electrochim. Acta* **2016**, *188*, 574–581. [[CrossRef](#)]
113. Crew, A.; Lonsdale, D.; Byrd, N.; Pittson, R.; Hart, J.P. A screen-printed, amperometric biosensor array incorporated into a novel automated system for the simultaneous determination of organophosphate pesticides. *Biosens. Bioelectron.* **2011**, *26*, 2847–2851. [[CrossRef](#)]
114. Arduini, F.; Guidone, S.; Amine, A.; Palleschi, G.; Moscone, D. Acetylcholinesterase biosensor based on self-assembled monolayer-modified gold-screen printed electrodes for organophosphorus insecticide detection. *Sens. Actuators B Chem.* **2013**, *179*, 201–208. [[CrossRef](#)]
115. De Albuquerque, Y.D.T.; Ferreira, L.F. Amperometric biosensing of carbamate and organophosphate pesticides utilizing screen-printed tyrosinase-modified electrodes. *Anal. Chim. Acta* **2007**, *596*, 210–221. [[CrossRef](#)]
116. Gogol, E.V.; Evtugyn, G.A.; Marty, J.; Budnikov, H.C.; Winter, V.G. Amperometric biosensors based on nafion coated screen-printed electrodes for the determination of cholinesterase inhibitors. *Talanta* **2000**, *53*, 379–389. [[CrossRef](#)]
117. Sajjadi, S.; Ghourchian, H.; Tavakoli, H. Choline oxidase as a selective recognition element for determination of paraoxon. *Biosens. Bioelectron.* **2009**, *24*, 2509–2514. [[CrossRef](#)]
118. Dounin, V.; Veloso, A.J.; Schulze, H.; Bachmann, T.T.; Kerman, K. Disposable electrochemical printed gold chips for the analysis of acetylcholinesterase inhibition. *Anal. Chim. Acta* **2010**, *669*, 63–67. [[CrossRef](#)]
119. Mayorga-Martinez, C.C.; Pino, F.; Kurbanoglu, S.; Rivas, L.; Ozkan, S.A.; Merkoçi, A. Iridium oxide nanoparticle induced dual catalytic/inhibition based detection of phenol and pesticide compounds. *J. Mater. Chem. B* **2014**, *2*, 2233–2239. [[CrossRef](#)]
120. Catalina, D.; Carvajal, S.; Peñuela, G. Effect of chlorpyrifos on the inhibition of the enzyme acetylcholinesterase by cross-linking in water-supply samples and milk from dairy cattle. *Talanta* **2013**, *111*, 1–7. [[CrossRef](#)]
121. Chen, D.; Liu, Z.; Fu, J.; Guo, Y.; Sun, X.; Yang, Q.; Wang, X. Electrochemical acetylcholinesterase biosensor based on multi-walled carbon nanotubes/dicyclohexyl phthalate modified screen-printed electrode for detection of chlorpyrifos. *J. Electroanal. Chem.* **2017**, *801*, 185–191. [[CrossRef](#)]
122. Shi, Q.; Teng, Y.; Zhang, Y.; Liu, W. Rapid detection of organophosphorus pesticide residue on Prussian blue modified dual-channel screen-printed electrodes combing with portable potentiostat. *Chin. Chem. Lett.* **2018**, *29*, 1379–1382. [[CrossRef](#)]
123. Domínguez-renedo, O.; Alonso-lomillo, M.A.; Recio-cebrían, P.; Arcos-martínez, M.J. Screen-printed acetylcholinesterase-based biosensors for inhibitive determination of permethrin. *Sci. Total Environ.* **2012**, *426*, 346–350. [[CrossRef](#)]
124. Jin, R.; Kong, D.; Zhao, X.; Li, H.; Yan, X.; Liu, F.; Sun, P.; Du, D.; Lin, Y.; Lu, G. Tandem catalysis driven by enzymes directed hybrid nanoflowers for on-site ultrasensitive detection of organophosphorus pesticide. *Biosens. Bioelectron.* **2019**, *141*, 111473. [[CrossRef](#)]
125. Arduini, F.; Forchielli, M.; Amine, A.; Neagu, D.; Cacciotti, I.; Nanni, F.; Moscone, D.; Palleschi, G. Screen-printed biosensor modified with carbon black nanoparticles for the determination of paraoxon based on the inhibition of butyrylcholinesterase. *Microchim. Acta* **2014**, *182*, 643–651. [[CrossRef](#)]
126. Gan, N.; Yang, X.; Xie, D.; Wu, Y.; Wen, W. A disposable organophosphorus pesticides enzyme biosensor based on magnetic composite nano-particles modified screen printed carbon electrode. *Sensors* **2010**, *10*, 625–638. [[CrossRef](#)]
127. Ivanov, A.; Evtugyn, G.; Budnikov, H.; Ricci, F.; Moscone, D.; Palleschi, G. Cholinesterase sensors based on screen-printed electrodes for detection of organophosphorus and carbamic pesticides. *Anal. Bioanal. Chem.* **2003**, *377*, 624–631. [[CrossRef](#)]
128. Chen, D.; Jiao, Y.; Jia, H.; Guo, Y.; Sun, X.; Wang, X.; Xu, J. Acetylcholinesterase biosensor for chlorpyrifos detection based on multi-walled carbon nanotubes-SnO₂-chitosan nanocomposite modified screen-printed electrode. *Int. J. Electrochem. Sci.* **2015**, *10*, 10491–10501.

129. El-Moghazy, A.Y.; Soliman, E.A.; Ibrahim, H.Z.; Marty, J.L.; Istamboulie, G.; Noguer, T. Biosensor based on electrospun blended chitosan-poly (vinyl alcohol) nanofibrous enzymatically sensitized membranes for pirimiphos-methyl detection in olive oil. *Talanta* **2016**, *155*, 258–264. [[CrossRef](#)]
130. Zhang, Q.; Xu, Q.; Guo, Y.; Sun, X.; Wang, X. Acetylcholinesterase biosensor based on the mesoporous carbon/ferroferic oxide modified electrode for detecting organophosphorus pesticides. *RSC Adv.* **2016**, *6*, 24698–24703. [[CrossRef](#)]
131. Tang, W.; Fan, K.; Zhou, J.; Wu, J.; Ji, F. Unmodified screen-printed silver electrode for facile detection of organophosphorus pesticide. *Ionics* **2015**, *21*, 587–592. [[CrossRef](#)]
132. Joshi, K.A.; Tang, J.; Haddon, R.; Wang, J.; Chen, W.; Mulchandani, A. A disposable biosensor for organophosphorus nerve agents based on carbon nanotubes modified thick film strip electrode. *Electroanalysis* **2005**, *17*, 54–58. [[CrossRef](#)]
133. Sinha, R.; Ganesana, M.; Andreescu, S.; Stanciu, L. AChE biosensor based on zinc oxide sol-gel for the detection of pesticides. *Anal. Chim. Acta* **2010**, *661*, 195–199. [[CrossRef](#)]
134. Bonnet, C.; Andreescu, S.; Marty, J. Adsorption: An easy and efficient immobilisation of acetylcholinesterase on screen-printed electrodes. *Anal. Chim. Acta* **2003**, *481*, 209–211. [[CrossRef](#)]
135. Chen, D.; Fu, J.; Liu, Z.; Guo, Y.; Sun, X.; Wang, X.; Wang, Z. A Simple acetylcholinesterase biosensor based on ionic liquid/multiwalled carbon nanotubes-modified screen-printed electrode for rapid detecting chlorpyrifos. *Int. J. Electrochem. Sci.* **2017**, *12*, 9465–9477. [[CrossRef](#)]
136. Zhang, L.; Zhang, A.; Du, D.; Lin, Y. Biosensor based on Prussian blue nanocubes/reduced graphene oxide nanocomposite for detection of organophosphorus pesticides. *Nanoscale* **2012**, *4*, 4674–4679. [[CrossRef](#)]
137. Bucur, B.; Fournier, D.; Danet, A.; Marty, J.L. Biosensors based on highly sensitive acetylcholinesterases for enhanced carbamate insecticides detection. *Anal. Chim. Acta* **2006**, *562*, 115–121. [[CrossRef](#)]
138. Laschi, S.; Ogończyk, D.; Palchetti, I.; Mascini, M. Evaluation of pesticide-induced acetylcholinesterase inhibition by means of disposable carbon-modified electrochemical biosensors. *Enzyme Microb. Technol.* **2007**, *40*, 485–489. [[CrossRef](#)]
139. Del Carlo, M.; Mascini, M.; Pepe, A.; Compagnone, D.; Mascini, M. Electrochemical bioassay for the investigation of chlorpyrifos-methyl in vine samples. *J. Agric. Food Chem.* **2002**, *50*, 7206–7210. [[CrossRef](#)]
140. Li, Y.G.; Zhou, Y.X.; Feng, J.L.; Jiang, Z.H.; Ma, L.R. Immobilization of enzyme on screen-printed electrode by exposure to glutaraldehyde vapour for the construction of amperometric acetylcholinesterase electrodes. *Anal. Chim. Acta* **1999**, *382*, 277–282. [[CrossRef](#)]
141. Del Carlo, M.; Mascini, M.; Pepe, A.; Diletti, G.; Compagnone, D. Screening of food samples for carbamate and organophosphate pesticides using an electrochemical bioassay. *Food Chem.* **2004**, *84*, 651–656. [[CrossRef](#)]
142. Law, K.A.; Higson, S.P.J. Sonochemically fabricated acetylcholinesterase micro-electrode arrays within a flow injection analyser for the determination of organophosphate pesticides. *Biosens. Bioelectron.* **2005**, *20*, 1914–1924. [[CrossRef](#)]
143. Di Sioudi, B.D.; Miller, C.E.; Lai, K.; Grimsley, J.K.; Wild, J.R. Rational design of organophosphorus hydrolase for altered substrate specificities. *Chem. Biol. Interact.* **1999**, *119–120*, 211–223. [[CrossRef](#)]
144. Efremenko, E.N.; Sergeeva, V.S. Organophosphate hydrolase—An enzyme catalyzing degradation of phosphorus-containing toxins and pesticides. *Russ. Chem. Bull.* **2001**, *50*, 1826–1832. [[CrossRef](#)]
145. Shimazu, M.; Mulchandani, A.; Chen, W. Simultaneous degradation of organophosphorus pesticides and p-nitrophenol by a genetically engineered *Moraxella* sp. with surface-expressed organophosphorus hydrolase. *Biotechnol. Bioeng.* **2001**, *76*, 318–324. [[CrossRef](#)]
146. Chough, S.H.; Mulchandani, A.; Mulchandani, P.; Chen, W.; Wang, J.; Rogers, K.R. Organophosphorus Hydrolase-Based Amperometric Sensor: Modulation of Sensitivity and Substrate Selectivity. *Electroanalysis* **2002**, *14*, 273–276. [[CrossRef](#)]
147. Lei, Y.; Mulchandani, P.; Wang, J.; Chen, W.; Mulchandani, A. Highly sensitive and selective amperometric microbial biosensor for direct determination of p-nitrophenyl-substituted organophosphate nerve agents. *Environ. Sci. Technol.* **2005**, *39*, 8853–8857. [[CrossRef](#)]
148. Mulchandani, A.; Chen, W.; Mulchandani, P.; Wang, J.; Rogers, K.R. Biosensors for direct determination of organophosphate pesticides. *Biosens. Bioelectron.* **2001**, *16*, 225–230. [[CrossRef](#)]
149. Mulchandani, A. Amperometric Thick-Film Strip Electrodes for Monitoring Organophosphate Nerve Agents Based on Immobilized Organophosphorus Hydrolase. *Anal. Chem.* **1999**, *71*, 2246–2249. [[CrossRef](#)]

150. Joshi, K.A.; Prouza, M.; Kum, M.; Wang, J.; Tang, J.; Haddon, R.; Chen, W.; Mulchandani, A. V-type nerve agent detection using a carbon nanotube-based amperometric enzyme electrode. *Anal. Chem.* **2006**, *78*, 331–336. [[CrossRef](#)]
151. Zhao, Y.; Zhang, W.; Lin, Y.; Du, D. The vital function of Fe₃O₄@Au nanocomposites for hydrolase biosensor design and its application in detection of methyl parathion. *Nanoscale* **2013**, *5*, 1121–1126. [[CrossRef](#)]
152. Sacks, V.; Eshkenazi, I.; Neufeld, T.; Dosoretz, C.; Rishpon, J. Immobilized Parathion Hydrolase: An Amperometric Sensor for Parathion. *Anal. Chem.* **2000**, *72*, 2055–2058. [[CrossRef](#)]
153. Mulyasuryani, A.; Dofir, M. Enzyme Biosensor for Detection of Organophosphate Pesticide Residues Base on Screen Printed Carbon Electrode (SPCE)-Bovine Serum Albumin (BSA). *Engineering* **2014**, *6*, 230–235. [[CrossRef](#)]
154. Primožič, M.; Čolnik, M.; Knez, Ž.; Leitgeb, M. Advantages and disadvantages of using SC CO₂ for enzyme release from halophilic fungi. *J. Supercrit. Fluids* **2019**, *143*, 286–293. [[CrossRef](#)]
155. Brahim, M.B.; Belhadj Ammar, H.; Abdelhédi, R.; Samet, Y. Electrochemical behavior and analytical detection of Imidacloprid insecticide on a BDD electrode using square-wave voltammetric method. *Chin. Chem. Lett.* **2016**, *27*, 666–672. [[CrossRef](#)]
156. Zhang, M.; Zhao, H.T.; Xie, T.J.; Yang, X.; Dong, A.J.; Zhang, H.; Wang, J.; Wang, Z.Y. Molecularly imprinted polymer on graphene surface for selective and sensitive electrochemical sensing imidacloprid. *Sens. Actuators B Chem.* **2017**, *252*, 991–1002. [[CrossRef](#)]
157. Geto, A.; Safaa, J.; Mortensen, J.; Svendsen, W.E.; Dimaki, M. Electrochemical determination of bentazone using simple screen-printed carbon electrodes. *Environ. Int.* **2019**, *129*, 400–407. [[CrossRef](#)] [[PubMed](#)]
158. Della Pelle, F.; Angelini, C.; Sergi, M.; Del Carlo, M.; Pepe, A.; Compagnone, D. Nano carbon black-based screen printed sensor for carbofuran, isoprocarb, carbaryl and fenobucarb detection: Application to grain samples. *Talanta* **2018**, *186*, 389–396. [[CrossRef](#)] [[PubMed](#)]
159. Lezi, N.; Economou, A. Voltammetric Determination of Neonicotinoid Pesticides at Disposable Screen-Printed Sensors Featuring a Sputtered Bismuth Electrode. *Electroanalysis* **2015**, *27*, 2313–2321. [[CrossRef](#)]
160. Khairy, M.; Ayoub, H.A.; Banks, C.E. Non-enzymatic electrochemical platform for parathion pesticide sensing based on nanometer-sized nickel oxide modified screen-printed electrodes. *Food Chem.* **2018**, *255*, 104–111. [[CrossRef](#)] [[PubMed](#)]
161. Charoenkitamorn, K.; Chailapakul, O.; Siangproh, W. Development of gold nanoparticles modified screen-printed carbon electrode for the analysis of thiram, disulfiram and their derivative in food using ultra-high performance liquid chromatography. *Talanta* **2015**, *132*, 416–423. [[CrossRef](#)]
162. Zhang, C.; Zhao, F.; She, Y.; Hong, S.; Cao, X.; Zheng, L.; Wang, S.; Li, T.; Wang, M.; Jin, M.; et al. A disposable molecularly imprinted sensor based on Graphe@AuNPs modified screen-printed electrode for highly selective and sensitive detection of cyhexatin in pear samples. *Sens. Actuators B Chem.* **2019**, *284*, 13–22. [[CrossRef](#)]
163. Jubete, E.; Zelechowska, K.; Loaiza, O.A.; Lamas, P.J.; Ochoteco, E.; Farmer, K.D.; Roberts, K.P.; Biernat, J.F. Derivatization of SWCNTs with cobalt phthalocyanine residues and applications in screen printed electrodes for electrochemical detection of thiocholine. *Electrochim. Acta* **2011**, *56*, 3988–3995. [[CrossRef](#)]
164. Habekost, A. Rapid and sensitive spectroelectrochemical and electrochemical detection of glyphosate and AMPA with screen-printed electrodes. *Talanta* **2017**, *162*, 583–588. [[CrossRef](#)]
165. Karuppiah, C.; Palanisamy, S.; Chen, S.; Kannan, S.; Periakaruppan, P. A novel and sensitive amperometric hydrazine sensor based on gold nanoparticles decorated graphite nanosheets modified screen printed carbon electrode. *Electrochim. Acta* **2014**, *139*, 157–164. [[CrossRef](#)]
166. Thirumalraj, B.; Rajkumar, C.; Chen, S.; Lin, K. Determination of 4-nitrophenol in water by use of a screen-printed carbon electrode modified with chitosan-crafted ZnO nanoneedles. *J. Colloid Interface Sci.* **2017**, *499*, 83–92. [[CrossRef](#)] [[PubMed](#)]
167. Arvinte, A.; Mahosenaho, M.; Pinteala, M.; Sesay, A.M.; Virtanen, V. Electrochemical oxidation of p-nitrophenol using graphene-modified electrodes, and a comparison to the performance of MWNT-based electrodes. *Microchim. Acta* **2011**, *174*, 337–343. [[CrossRef](#)]
168. De Oliveira, R.; Amorim, É.; Rogério, A. Electrochemically activated multi-walled carbon nanotubes modified screen-printed electrode for voltammetric determination of sulfentrazone. *J. Electroanal. Chem.* **2019**, *835*, 220–226.

169. Sun, H.; Zhao, S.; Qu, F. Gold nanoparticles modified ceria nanoparticles for the oxidation of hydrazine with disposable screen-printed electrode. *Measurement* **2012**, *45*, 1111–1113. [[CrossRef](#)]
170. Pino, F.; Mayorga-Martinez, C.C.; Merkoçi, A. High-performance sensor based on copper oxide nanoparticles for dual detection of phenolic compounds and a pesticide. *Electrochem. Commun.* **2016**, *71*, 33–37. [[CrossRef](#)]
171. Saengsookwaow, C.; Rangkupan, R.; Chailapakul, O. Nitrogen-doped graphene-polyvinylpyrrolidone/gold nanoparticles modified electrode as a novel hydrazine sensor. *Sens. Actuators B Chem.* **2016**, *227*, 524–532. [[CrossRef](#)]
172. Chuntib, P.; Themsirimongkon, S.; Saipanya, S.; Jakmune, J. Sequential injection differential pulse voltammetric method based on screen printed carbon electrode modified with carbon nanotube/Nafion for sensitive determination of paraquat. *Talanta* **2017**, *170*, 1–8. [[CrossRef](#)]
173. Jirasirichote, A.; Punrat, E.; Suea-ngam, A.; Chailapakul, O. Voltammetric detection of carbofuran determination using screen-printed carbon electrodes modified with gold nanoparticles and graphene oxide. *Talanta* **2017**, *175*, 331–337. [[CrossRef](#)]
174. Govindasamy, M.; Mani, V.; Chen, S.M.; Chen, T.W.; Sundramoorthy, A.K. Methyl parathion detection in vegetables and fruits using silver@graphene nanoribbons nanocomposite modified screen printed electrode. *Sci. Rep.* **2017**, *7*, 46471. [[CrossRef](#)]
175. Arduini, F.; Cassisi, A.; Amine, A.; Ricci, F.; Moscone, D.; Palleschi, G. Electrocatalytic oxidation of thiocholine at chemically modified cobalt hexacyanoferrate screen-printed electrodes. *J. Electroanal. Chem.* **2009**, *626*, 66–74. [[CrossRef](#)]
176. Mehta, J.; Vinayak, P.; Tuteja, S.K.; Chhabra, V.A.; Bhardwaj, N.; Paul, A.K.; Kim, K.; Deep, A. Graphene modified screen printed immunosensor for highly sensitive detection of parathion. *Biosens. Bioelectron.* **2016**, *83*, 339–346. [[CrossRef](#)] [[PubMed](#)]
177. Mehta, J.; Bhardwaj, N.; Bhardwaj, S.K.; Tuteja, S.K.; Vinayak, P.; Paul, A.K.; Kim, K.; Deep, A. Graphene quantum dot modified screen printed immunosensor for the determination of parathion. *Anal. Biochem.* **2017**, *523*, 1–9. [[CrossRef](#)] [[PubMed](#)]
178. Dzantiev, B.B.; Yazynina, E.V.; Zherdev, A.V.; Plekhanova, Y.V.; Reshetilov, A.N.; Chang, S.; Mcneil, C.J. Determination of the herbicide chlorsulfuron by amperometric sensor based on separation-free bienzyme immunoassay. *Sens. Actuators B Chem.* **2004**, *98*, 254–261. [[CrossRef](#)]
179. Pérez-Fernández, B.; Mercader, J.V.; Checa-Orrego, B.I.; de la Escosura-Muñiz, A.; Costa-García, A. A monoclonal antibody-based immunosensor for the electrochemical detection of imidacloprid pesticide. *Analyst* **2019**, *144*, 2936–2941. [[CrossRef](#)]
180. Pérez-fernández, B.; Mercader, J.V.; Abad-fuentes, A.; Brenda, I.; De Escosura-muñiz, A.; Costa-garcía, A. Direct competitive immunosensor for Imidacloprid pesticide detection on gold nanoparticle-modified electrodes. *Talanta* **2019**, *209*, 120465. [[CrossRef](#)]
181. Wei, W.; Zong, X.; Wang, X.; Yin, L.; Pu, Y.; Liu, S. A disposable amperometric immunosensor for chlorpyrifos-methyl based on immunogen/platinum doped silica sol – gel film modified screen-printed carbon electrode. *Food Chem.* **2012**, *135*, 888–892. [[CrossRef](#)]
182. Grennan, K.; Strachan, G.; Porter, A.J.; Killard, A.J.; Smyth, M.R. Atrazine analysis using an amperometric immunosensor based on single-chain antibody fragments and regeneration-free multi-calibrant measurement. *Anal. Chim. Acta* **2003**, *500*, 287–298. [[CrossRef](#)]
183. Skla, P. The immunosensors for measurement of 2, 4-dichlorophenoxyacetic acid based on electrochemical impedance spectroscopy. *Bioelectrochemistry* **2004**, *62*, 11–18.
184. Stoltenburg, R.; Reinemann, C.; Strehlitz, B. SELEX—A (r) evolutionary method to generate high-affinity nucleic acid ligands. *Biomol. Eng.* **2007**, *24*, 381–403. [[CrossRef](#)]
185. Madianos, L.; Tsekenis, G.; Skotadis, E.; Patsiouras, L.; Tsoukalas, D. A highly sensitive impedimetric aptasensor for the selective detection of acetamiprid and atrazine based on microwires formed by platinum nanoparticles. *Biosens. Bioelectron.* **2018**, *101*, 268–274. [[CrossRef](#)]
186. Madianos, L.; Skotadis, E.; Tsekenis, G.; Patsiouras, L.; Tsigkourakos, M.; Tsoukalas, D. Impedimetric nanoparticle aptasensor for selective and label free pesticide detection. *Microelectron. Eng.* **2018**, *189*, 39–45. [[CrossRef](#)]
187. Jiao, Y.; Hou, W.; Fu, J.; Guo, Y.; Sun, X. A nanostructured electrochemical aptasensor for highly sensitive detection of chlorpyrifos. *Sens. Actuators B Chem.* **2017**, *243*, 1164–1170. [[CrossRef](#)]

188. Rapini, R.; Marrazza, G. Electrochemical aptasensors for contaminants detection in food and environment: Recent advances. *Bioelectrochemistry* **2017**, *118*, 47–61. [[CrossRef](#)] [[PubMed](#)]
189. Erdem, A.; Eksin, E.; Muti, M. Chitosan—Graphene oxide based aptasensor for the impedimetric detection of lysozyme. *Colloids Surfaces B Biointerfaces* **2014**, *115*, 205–211. [[CrossRef](#)]
190. Wang, C.; Chen, B.; Zou, M.; Cheng, G. Cyclic RGD-modified chitosan / graphene oxide polymers for drug delivery and cellular imaging. *Colloids Surfaces B Biointerfaces* **2014**, *122*, 332–340. [[CrossRef](#)]
191. Liu, M.; Khan, A.; Wang, Z.; Liu, Y.; Yang, G.; Deng, Y.; He, N. Aptasensors for pesticide detection. *Biosens. Bioelectron.* **2019**, *130*, 174–184. [[CrossRef](#)]
192. Fei, A.; Liu, Q.; Huan, J.; Qian, J.; Dong, X.; Qiu, B.; Mao, H.; Wang, K. Label-free impedimetric aptasensor for detection of femtomole level acetamiprid using gold nanoparticles decorated multiwalled carbon nanotube-reduced graphene oxide nanoribbon composites. *Biosens. Bioelectron.* **2015**, *70*, 122–129. [[CrossRef](#)]
193. Rapini, R.; Cincinelli, A.; Marrazza, G. Acetamiprid multidetection by disposable electrochemical DNA aptasensor. *Talanta* **2016**, *161*, 15–21. [[CrossRef](#)]
194. Fu, J.; An, X.; Yao, Y.; Guo, Y.; Sun, X. Electrochemical aptasensor based on one step co-electrodeposition of aptamer and GO-CuNPs nanocomposite for organophosphorus pesticide detection. *Sens. Actuators B Chem.* **2019**, *287*, 503–509. [[CrossRef](#)]
195. Hassani, S.; Akmal, M.R.; Salek-Maghsoudi, A.; Rahmani, S.; Ganjali, M.R.; Norouzi, P.; Abdollahi, M. Novel label-free electrochemical aptasensor for determination of Diazinon using gold nanoparticles-modified screen-printed gold electrode. *Biosens. Bioelectron.* **2018**, *120*, 122–128. [[CrossRef](#)] [[PubMed](#)]
196. Mulchandani, A.; Mulchandani, P.; Chauhan, S.; Kaneva, I.; Chen, W. A Potentiometric Microbial Biosensor for Direct Determination of Organophosphate Nerve Agents. *Electroanalysis* **1998**, *10*, 733–737. [[CrossRef](#)]
197. Chen, W.; Mulchandani, A. Flow Injection Amperometric Enzyme Biosensor for Direct Determination of Organophosphate Nerve Agents. *Environ. Sci. Technol.* **2001**, *35*, 2562–2565.
198. Mulchandani, P.; Mulchandani, A.; Kaneva, I.; Chen, W. Biosensor for direct determination of organophosphate nerve agents. 1. Potentiometric enzyme electrode. *Biosens. Bioelectron.* **1999**, *14*, 77–85. [[CrossRef](#)]
199. Touloupakis, E.; Giannoudi, L.; Piletsky, S.A.; Guzzella, L.; Pozzoni, F.; Giardi, M.T. A multi-biosensor based on immobilized Photosystem II on screen-printed electrodes for the detection of herbicides in river water. *Biosens. Bioelectron.* **2005**, *20*, 1984–1992. [[CrossRef](#)] [[PubMed](#)]
200. Chatzipetrou, M.; Milano, F.; Giotta, L.; Chirizzi, D.; Trotta, M.; Massaouti, M.; Guascito, M.R.; Zergioti, I. Functionalization of gold screen printed electrodes with bacterial photosynthetic reaction centers by laser printing technology for mediatorless herbicide biosensing. *Electrochem. Commun.* **2016**, *64*, 46–50. [[CrossRef](#)]
201. Kumar, J.; Souza, S.F.D. Microbial biosensor for detection of methyl parathion using screen printed carbon electrode and cyclic voltammetry. *Biosens. Bioelectron.* **2011**, *26*, 4289–4293. [[CrossRef](#)]

